Table 2. Copolymerization of Vinylated Heparin and Styrenated Gelatin and Their Photocuring Characteristics[a]

styrenated gelatin[b] (wt %)	heparin (wt %) methacrylate (A)[e]	methacrylate (B)[c,f]	styrenated[d]	total concn (wt %)	gel yield (%)	fegree of swelling
10	30			40	12 ± 1	22 ± 2
20	20			40	50 ± 3	10 ± 3
30	10			40	75 ± 1	5 ± 1
5		30		35	21 ± 1	17 ± 2
30		5		35	68 ± 5	8 ± 1
10			10	20	93 ± 1	8 ± 2
20			10	30	93 ± 3	7 ± 2
30			10	40	91 ± 1	3 ± 0.5
10			20	30	97 ± 3	4 ± 0.5
20			20	40	84 ± 1	4 ± 1
10			30	40	98 ± 0.5	4 ± 1

[a] Photointensity, 200 mW/cm²; photoirradiation time, 5 min; photoinitator, 0.5 wt % to monomer. Number of experiments, $n > 3$. [b] Number of derivatized groups (per molecule): styrene group, 25.5. [c] Number of derivatized groups (per molecule): methacryl group, 1.9. [d] Number of derivatized groups (per molecule): styrene group, 9.7. [e] Methacrylate (A): methacrylate derivatized on the terminus. [f] Methacrylate (B): methacrylate derivatized on the side chain.

Table 3. Copolymerization of Vinylated Heparin with Other Vinylated Biomolecules and Their Photocuring Characteristics[a]

heparin (wt %) methacrylate (A)[b]	styrenated (B)[b]	styrenated gelatin (C)[b] (wt %)	styrenated albumin (D)[b] (wt %)	styrenated chitosan (E)[b] (wt %)	styrenated hyaluronan (F)[b] (wt %)	total concn (wt %)	gel yield (%)	degree of swelling
3		20 (a)	3	3		29	74 ± 2	13 ± 3
20			5			25	2	93 ± 20
	5	5 (a)	10			20	89 ± 3	21 ± 3
	5	10 (a)	5			20	89 ± 3	12 ± 1
	9.5	9.5 (b)			1	20	85 ± 5	10 ± 3
	10			10		20	59 ± 2	22 ± 5
	19				1	20	90 ± 1	10 ± 1

[a] Photointensity, 200 mW/cm²; photoirradiation time, 5 min; photoinitator, 0.5 wt % to monomer. Number of experiments, $n > 3$. [b] Number of derivatized groups (per molecule): (A) methacryl group 1.9; (B) styrene group, 9.7; (C) styrene group, (a) 25.5, (b) 30.0; (D) styrene group, 15.5; (E) styrene group, 2.9; (F) styrene group, 24.8.

mechanical and physical properties. For example, a heparin–gelatin copolymer may serve as a tissue-and blood-compatible ECM, which is due to potent anticoagulant activity derived from incorporated heparin.

The results of copolymerization of methacrylated or styrenated heparin and styrenated gelatin are shown in Table 2. When the total feed monomer concentration in the copolymerization of styrenated gelatin and terminally monomethacrylated heparin was fixed at 40 wt %, an increase in the concentration of monomethacrylated heparin resulted in a decreased gel yield and an increased degree of swelling. On the other hand, copolymerization of styrenated gelatin and styrenated heparin gave almost 91–98% yield, regardless of the mixing ratio and the total feed monomer concentration in the range investigated (20–40 wt %). The degree of swelling of copolymers of styrenated heparin and styrenated gelatin remained relatively low (approximately 3–8) as compared with those of copolymers of methacrylated heparin and styrenated gelatin.

The results of copolymerization of vinylated heparin and other various vinylated biomolecules such as styrenated albumin, styrenated chitosan, and styrenated hyluronan are shown in Table 3. Copolymerization of methacrylated heparin and styrenated albumin produced an extremely low gel yield. On the other hand, copolymerization of styrenated heparin and other styrenated biomacromolecules such as gelatin, albumin, chitosan, and hyaluronan (5 wt % monomer feed) produced relatively high gel yields (60–90%). The degrees of swelling ranged from 10 to 20. Irrespective of homopolymer or copolymer, the resultant gels were transparent and elastomeric except for copolymers with high degrees of swelling.

Microscopic Structure of Photocured Films. SEM images of the interior structures of freeze-dried photocured gels that were mechanically broken are shown in Figure 5. Photocured gels prepared from methacrylated heparin or styrenated hyaluronan were composed of a random network of fibrous structures. On the other hand, for gels prepared from styrenated heparin, an increase in the degree of derivatization resulted in a smaller size of the honeycomb structure (interspace; a few to several tenths micrometer, depending on the degree of derivatization). Gels prepared from styrenated gelatin or styrenated albumin exhibited an irregular honeycomb-like structure (pore size was about 10 μm). A chitosan gel produced regularly ordered, small honeycomb structures (pore size was about 3 μm).

Tubular Photoconstructs. Tubular photoconstructs were prepared by pouring an aqueous mixture of vinylated biomacromolecules and CQ-COOH into the interspace of a mold consisting of a glass mandrel (mold A = 2.5 mm outer diameter or mold B = 4.0 mm outer diameter) and a silicone sheath (mold A = 1.4 mm inner diameter or mold B = 2.0 mm inner diameter) (Figure 2), and subsequent photoirradiation under rotation for 5 min. Tubular photoconstructs prepared from a mixture of styrenated gelatin (30 wt %) and methacrylated heparin (5 wt %) using the mold A (Figure

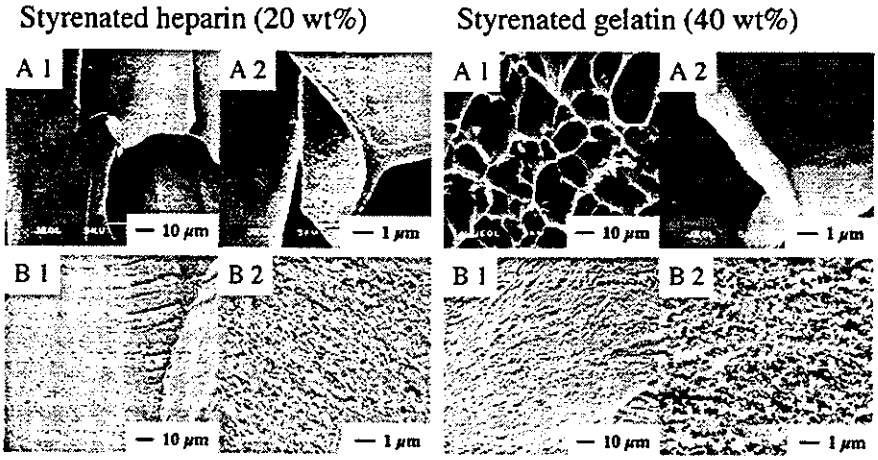

Figure 5. SEM images of photocured styrenated heparin gel and gelatin gel (5 min of irradiation at 200 mW/cm^2): (A) freeze-drying at −70 °C for 1 h; (B) graded ethanol dehydration and subsequent critical point drying. Original magnification: (1) ×1000; (2) ×10000.

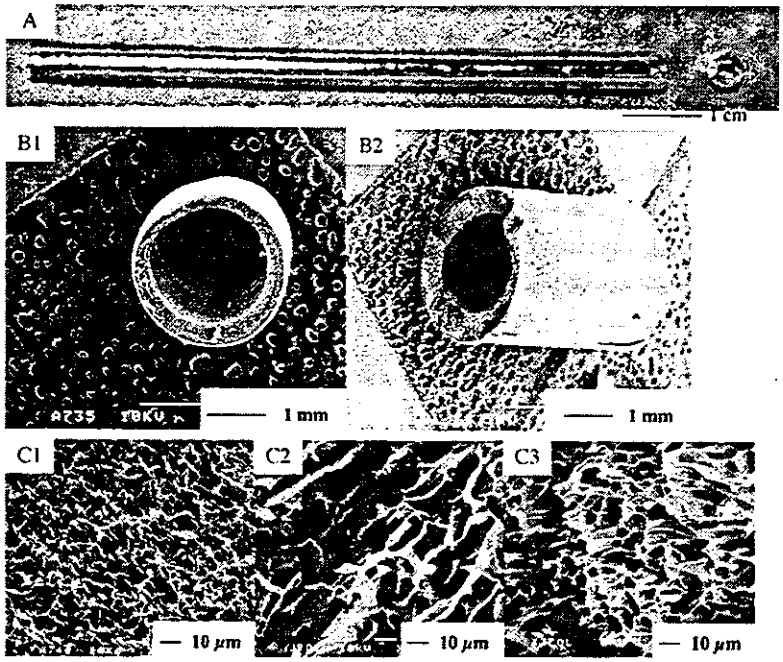

Figure 6. Photographs of tubular photoconstructs produced by vinylated biomolecules: (A) photograph of an as-prepared tube and its cross section; (B) SEM photos of freeze-dried tube; (B1) top view; (B2) side view; (C) SEM images of cross section of tubes at high magnification. The formulation of tube formation: (A and C3) gel composed of styrenated gelatin (20 wt %), styrenated heparin (2 wt %), and PEGDA400 (5 wt %), (B1 and C1) gel composed of styrenated gelatin (30 wt %) and methacrylated heparin (5 wt %); (C2) gel composed of styrenated gelatin (10 wt %) and styrenated heparin (10 wt %).

6B1,C1) and a mixture of styrenated gelatin (20 wt %), styrenated heparin (2 wt %), and diacrylated poly(ethylene glycol) (PEGDA400, 5 wt %), using mold B (Figure 6A,B2,C3) were produced upon visible light irradiation under rotation of the mold. The resultant tubes (designated as tube A and tube B, respectively) were transparent, elastomeric, and soft. The as-prepared gel in mold A had an inner diameter of 1.8 mm and an outer diameter of 2.3 mm, and that in mold B had 2.6 and 3.6 mm, respectively.

These tubes were frozen at different temperatures (−20, −70, and −150 °C) and subsequently dried under vacuum. SEM revealed that irrespective of the freeze-drying temperature, luminal surfaces were nonpermeable although some micropatterns were formed, but microporous structures were formed on the outer surface of the tubes irrespective of type of tube and the freezing temperature (Figures 7 and 8). The tubes that were frozen at −20 °C and subsequently dried under vacuum were very fragile and often broke when held by hand. On the other hand, tubes subjected to freezing at −150 °C and subsequent drying under vacuum were tough. Fine porous structures were obtained for both tubes upon freezing at −70 °C.

The increase in intraluminal pressure upon infusion of water into a tube resulted in the expansion of the tube diameter, and with further increase of luminal pressure, the tubes broke. Table 4 lists the breaking pressure, the diameter change, and the calculated compliance. Breaking pressures were low (approximately 20−40 mmHg), irrespective of the type of tube and with or without freeze-drying. The change in diameter at the breaking pressure was approximately 20%

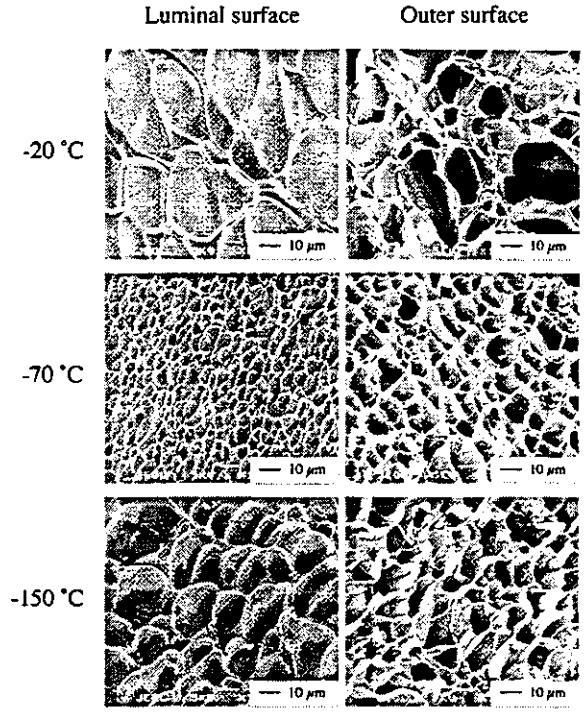

Figure 7. SEM images of freeze-dried tubular photoconstructs produced from a mixture of styrenated gelatin (20 wt %) and PEGDA400 (5 wt %) at different freezing temperatures.

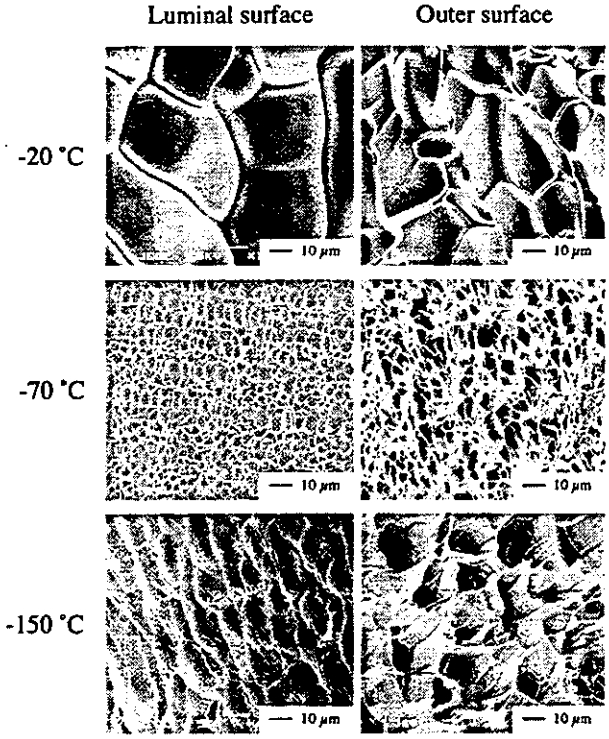

Figure 8. SEM images of freeze-dried tubular photoconstructs produced from a mixture of styrenated gelatin (20 wt %), styrenated heparin (2 wt %), and PEGDA400 (5 wt %) at different freezing temperatures.

for tube A and 13−14% for tube B. Taking these values together with the calculated compliance, it may be concluded that tube B was slightly less compliant than tube A.

Discussion

The utilization of naturally occurring biomacromolecules in biomedical applications has been increasingly demanded as fundamental materials for drug-loading matrixes, cell-adhesive or non-cell-adhesive coatings, and cell-immobilizable extracellular matrixes and scaffolds. Most of these naturally occurring biomacromolecules are soluble in water. To use them in the solid or hydrogel form, cross-linking via physical or chemical processes is required. Although much effort has been exerted for cross-linking using condensation reagents, our technology to this end is photochemically driven cross-linking and fabrication. The photochemistries utilized are [2 + 2] cyclo dimerization reactions and radical recombination reactions leading to inter- and intramolecular cross-linking, and radical polymerization. The first class of photoreactive groups used consists of cinnamate, coumarin, and thymine, the second class includes phenyl azide, dithiocarbamate, and benzophenon, and the third class includes radically polymerizable vinyl groups such as styryl or (meth)acryloyl groups. In our previous paper,[8] we have prepared photopolymerizable gelatin and albumin, both of which are partially derivatized with styrene groups, and then polymerized in the presence of water-soluble camphorquinone as a radical producing agent under visible light irradiation.

Previous research on a series of vinylated polysaccharides[11,12] by Hennink and his colleagues includes the preparation of methacrylated dextran (glycidyl methacrylate derivatized dextran) with or without a hydrolytically labile spacer, oligolactate and redox polymerization of aqueous solution containing methacrylated dextran and drug. These polym-

Table 4. Preparation of Tubular Photoconstructs and Their Intraluminal Pressure-Mechanical Property Relations of Untreated and Freeze-Dried Samples

	solution composition (wt %)				dimensions (mm)					
tube	styrenated gelatin[a]	styrenated heparin[b]	PEGDA400[c]	state[d]	wall thickness	inner diameter	sample no.	breaking pressure (mmHg)	diameter change[e] (%)	compliance ($mmHg^{-1}$)[f]
A	20		5	wet	0.6	3.9 ± 0.2	$n = 8$	20.7 ± 0.2	19.8 ± 7.4	0.023 ± 0.017
				freeze-dried at −150 °C/wet	0.5	3.5 ± 0.3	$n = 5$	26.0 ± 8.8	20.8 ± 4.8	0.015 ± 0.005
B	20	2	5	wet	0.5	3.6 ± 0.1	$n = 8$	40.9 ± 19.1	13.1 ± 4.4	0.007 ± 0.002
				freeze-dried at −150 °C/wet	0.4	3.5 ± 0.2	$n = 6$	25.3 ± 8.0	14.7 ± 6.3	0.014 ± 0.009

[a] Number of styrene groups (per molecule), 25.5. [b] Number of styrene groups (per molecule), 9.7. [c] Diacrylated PEG (PEG segment, mol wt 400). [d] Wet: untreated, freeze-dried at −150 °C/wet; freeze-dried at −150 °C and equilibrated in water. [e] Diameter change (%) = ΔD (diameter change)/D_0 (initial diameter) × 100. [f] Compliance = 2 $\Delta D/D_0 \times 1/\Delta P$ (breaking pressure).

erized dextrans form biodegradable hydrogels for drug delivery matrixes.

In this study, we extended our vinylated biomacromolecule chemistry and photofabrication technology to polysaccharides including heparin, which is the most effective anticoagulant as well as hyaluronan and chitosan. Scaffolds or templates for artificial devices and tissue-engineered devices are made of either naturally occurring biomacromolecules, synthetic polymers, or their hybrid composites. Biomacromolecules frequently used for biomedical technology include two different types: one is proteins and peptides, such as collagen (and its thermally denatured form, gelatin), albumin, fibronectin, and its cell active fragment; the other is polysaccharides, including hyaluronan, chitosan, and heparin. Both types of biomacromolecules are biodegradable, biosorbable, and nontoxic in nature. Since all these biomacromolecules are very soluble in water, fabrication to the desired forms requires solution-to-gel transformation by chemical or physical processes for use as cell adhesive or structural scaffold, bioactive substance-immobilized matrix, cell-inoculated matrix, or complexly shaped devices. Although a number of such processes leading to gelation have been employed, these methods are not useful for fabricating 3-D shaped constructs. Our ongoing research using 3-D macro-photoconstructs or stereolithographycally prepared microarchitecture of vinylated biomacromolecules including nerve tubular conduct packed with guide photocured fibers will verify that these photofabrication technologies using photoreactive biomacromolecules are really useful and effective for vital functioning hybrid tissues which are expected to repair or regenerate the lost or diseased living tissues.

Acknowledgment. This study was financially supported by the Promotion of Fundamental Studies in Health Science of the Organization for Pharmaceutical Safety and Research (OPSR) under Grant No. 97-15, and in part by a Grant-in-Aid for Scientific Research (A2-12358017, B2-12470277) from Ministry of Education, Culture, Sports, Science, and Technology of Japan. This study was partially performed at the Collaborative Center, Kyushu University.

References and Notes

(1) Langer, R. P.; Vacanti, J. P. *Tissue Eng. Sci.* **1993**, *260*, 920−926.
(2) Hubbell, J. A. *Mater. Res. Soc. Bidl.* **1996**, *21*, 33−35.
(3) Kim, B. S.; Mooney, D. J. *Trends Biotechnol.* **1998**, *16*, 224−230.
(4) Matsuda, T.; Miwa, H.; Moghaddam, M. J.; Iida, F. *ASAIO J.* **1993**, *39* (3), M327−31.
(5) Moghaddam, M. J.; Matsuda, T. *J. Polym. Sci., Chem. Ed.* **1993**, *A31*, 1589−1597.
(6) Sugawara, T.; Matsuda, T. *J. Biomed. Mater. Res.* **1996**, *32*, 157−164.
(7) Doi, K.; Nakayama, Y.; Matsuda, T. *J. Biomed. Mater. Res.* **1996**, *31*, 27−33.
(8) Nakayama, Y.; Okuda, K.; Matsuda, T. In preparation.
(9) Okino, H.; Nakayama, Y.; Tanaka, M.; Matsuda, T. *J. Biomed. Mater. Res.* **2002**, *59*, 233−245.
(10) Kim, S. H.; Chu, C. C. *J. Biomed. Mater. Res.* **2000**, *49*, 517−527.
(11) Hennink, W. E.; Talsma, H.; Borchert, J. C. H. *J. Controlled Release* **1996**, *39*, 47−55.
(12) Van Dijk-Wolthuis, W. N. E.; Franssen, O.; Talsma, H.; Van Steenbergen, M. J.; Van der Bosch, J. J. K.; Hennink, W. E. *Macromolecules* **1995**, *28*, 6317−6322.
(13) Van Dijk-Wolthuis, W. N. E.; Van steenbergen, M. J.; Underberg, W. J. M.; Hennink, W. E. *J. Pharm. Sci.* **1995**, *86* (4), 413−417.
(14) Smeds, K. A.; Grinstaff, M. W. *J. Biomed. Mater. Res.* **2001**, *54*, 115−121.
(15) Han, D. K.; Hullell, J. A. *Macromolecules* **1997**, *30*, 6077−6083.
(16) Vyavahare, N.; Kohn, J. *J. Polym. Sci., A: Polym. Chem.* **1994**, *32*, 1271−1281.
(17) Matsuda, T.; Magoshi, T. *Biomacromolecules* **2001**, *2* (4), 1169−1177.
(18) Nakayama, Y.; Mukai, T.; Hirano, Y.; Matsuda, T. In preparation.
(19) Hayashi, K.; Handa, H.; Nagasawa, S.; Okumura, A.; Moritake, K. *J. Biomech.* **1980**, *12*, 175−184.
(20) Sonoda, H.; Takamizawa, K.; Nakayama, Y.; Yasui, H.; Matsuda, T. *J. Biomed. Mater. Res.* **2001**, *55*, 266−276.
(21) Habeeb, A. F. *Anal. Biochem.* **1966**, *14*, 328−336.

BM0200229

Formation of Polymerized Mixed Heparin/Albumin Surface Layer and Cellular Adhesional Responses

Tomoko Magoshi† and Takehisa Matsuda*,‡

Department of Bioengineering, National Cardiovascular Center Research Institute, 5-7-1, Fujishirodai, Suita, Osaka, 565-8565, Japan, and Department of Biomedical Engineering, Graduate School of Medicine, Kyushu University, 3-1-1, Maidashi, Higashiku, Fukuoka 812-8562, Japan

Received March 25, 2002; Revised Manuscript Received June 3, 2002

The aim of this study was to create a dense albuminated layer, a heparinized layer, and a mixed layer on a poly(acrylic acid)-grafted surface via visible light induced photopolymerization. The procedure is comprised of four reaction steps: first, by visible light irradiation, acrylic acid (AA) was graft-polymerized on a segmented polyurethane (SPU) film that was preimpregnated with camphorquinone. The second step was adsorption of multiply styrenated albumin or styrenated heparin or their mixture, followed by visible light irradiation in the presence of carboxylated camphorquinone. The third step was covalent bonding between polyAA graft chain and polymerized biomacromolecule and between polymerized biomacromolecule to enforce the formation of a stable immobilized multilayer. X-ray photoelectron spectroscopic and Fourier transform-infrared spectroscopic measurements were conducted to analyze the surfaces formed at each step. Confocal laser scanning microscopy was utilized to determine the thickness of the biomacromolecule-immobilized layer with several tenths of a micrometer thickness. Platelet adhesion was markedly reduced on polymerized albuminated, polymerized heparinized, and copolymerized layers, whereas adhesive and proliferative potentials of endothelial cells, which were comparable to those of commercial tissue culture dishes, were observed on these surfaces. Co-immobilization of fibronectin and basic fibroblast growth factor enhanced these potentials. These densely multilayered surfaces may be suitable for artificial and tissue-engineered devices.

Introduction

The natural design of two-dimensional (D) extracellular surface (for example, basement membrane) and 3-D extracellular space in tissues is accomplished by supramolecular assemblies of biomacromolecules including proteins, proteoglycans, and immobilized cytokines. For 2-D extracellular design, various methods of preparing protein- and polysaccharide-bound matrixes have been devised and tested, since a biocompatible surface design determines the fate of implanted devices. Regardless of tissue- or blood-compatible surface design, protein monolayering or polysaccharide derivatization has often been employed via chemical methods or simply physical adsorption driven by either via electrostatic or hydrophobic interaction. Examples are given as heparin-bounding,[1−4] heparin-immmobilization,[5] alkylated heparin adsorption,[6] albumin immobilization,[7,8] and albumin−heparin conjugate immobilization.[9−12] On the other hand, a natural basement membrane is relatively thick. For example, the basement membrance of endothelium of a vascular graft is composed of dense meshes of supramolecularly assembled extracellular matrixes (ECMs).[13] On the other hand, long-term-driven artificial hearts had thrombus-free blood contacting surface which is covered by a dense proteinaceous layer, which appears to help prevent thrombus formation.[14] Tissue-engineered devices require a 3-D matrix for cell entrapment and proliferation, as well as phenotype restoration or redifferentiation of dedifferentiated cells due to monolayer culture in vitro. Therefore, one promising approach to acquire tissue and blood compatibility and tissue-regeneration surface activity may be to construct a dense multilayer composed of proteins, polysaccharides, and other bioactive substances such as cytokines on surfaces. The functional surface design of biomedical devices has often been achieved by surface hydrogelation, in which a hydrogel layer is covalently fixed on the surface, and a biologically active substance immobilized in the hydrogel undergoes sustained-release with time, thus enhancing surface bioactivity such as anticoagulation, cell adhesivity, vascularization, or minimal encapsulation leading to blood- or tissue-compatible surfaces. Albuimn−heparin multilayerly assembled coatings developed by Brynda,[10,11] which were prepared by alternative step-by-step layering of albumin and heparin and its covalent fixing, effectively functioned well as thromboresistant coating in vitro as well as in vivo.

In this article, the authors propose a novel technique for the formation of a densely packed protein- or heparin-polymerized surface layer via visible light induced surface photopolymerization, which requires four reaction steps as shown in Figure 1: Segmented polyurethane (SPU) film was used as a substrate. The first reaction is surface photograft

* To whom correspondence should be addressed: E-mail: matsuda@med.kyushu-u.ac.jp.
† National Cardiovascular Center Research Institute.
‡ Kyushu University.

10.1021/bm0200377 CCC: $22.00
Published on Web 07/17/2002

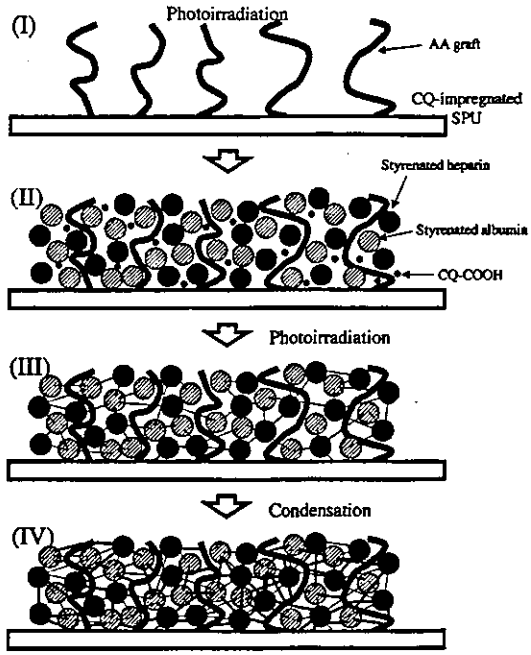

Figure 1. Schematic illustration of preparation of styrenated albumin and styrenated heparin copolymerized surface layer on SPU: (I) surface photograft polymerization to from polyAA-grafted surface; (II) soaking and absorption of a mixed solution of styrenated albumin, styrenated heparin and CQ-COOH; (III) photoirradiation by visible light; (IV) coupling reaction using a condensation regent.

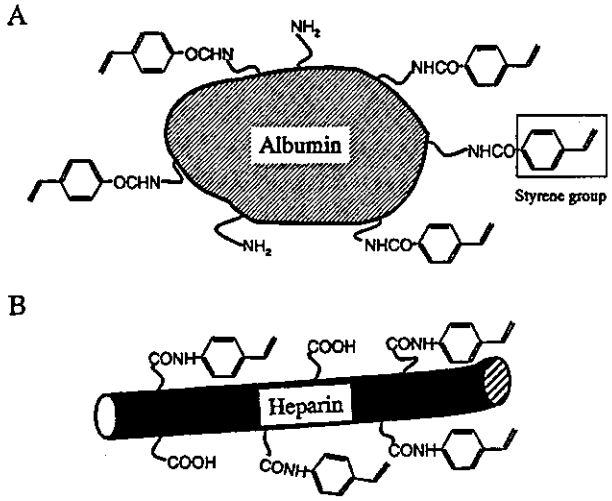

Figure 2. Schematic structures of styrenated albumin (A) and styrenated heparin (B).

polymerization of acrylic acid (AA) on SPU film which was impregnated with camphorquinone (CQ, a visible light induced radial producer) prior to photopolymerization. This technique was developed by us previously.[15] The resultant surface region was characteristic of a semi-interpenetrating network (s-IPN) structure composed of polyAA and substrate polymer, which produces a quite thick, water-swollen layer. The second step is "adsorption" of vinylated heparin and vinylated albumin on and "absorption" into the polyAA-grafted layer. These styrenated albumin and styrenated heparin (Figure 2) are prepared by partial condensation of the amino or carboxylic group present in the biomacromolecules with 4-vinylbenzoic acid (for albumin)[16] and 4-vinylaniline (for heparin)[17] according to our previous methods. The third step is photopolymerization in the presence of a water-soluble carboxylated CQ. The last step is covalent bonding between polyAA-grafted chains and these polymerized biomacromolecules and between polymerized biomacromolecules in the presence of a water-soluble condensation agent to form stable and dense multilayered biomacromolecular assemblies covalently fixed on the polymer surface. The cellular responses on such mixed heparin- and albumin-polymerized layers were determined, and the potential use of this polymerized biomacromolecule layering is discussed.

Materials and Methods

Materials. All solvents and reagents including camphorquinone (CQ) and Coomassie brilliant blue G-250 (CBBG) were purchased from Wako Pure Chemicals Inc. (Osaka, Japan). Acrylic acid (AA) was distilled under reduced pressure prior to use. 1-Ethyl-3-(dimethylaminopropyl)carbodiimide hydrochloride (WSC) was obtained from Dojindo Laboratory (Kumamoto, Japan). 5-(4,6-Dichlorotriazin-2-yl)aminofluorescein (DTAF), malachite green, and toluidine blue were purchased from Sigma Chemical Co. (St. Louis, MO). The SPU film (500 μm thickness) was obtained from Shedam Company (Osaka, Japan). Styrenated heparin (molecular weight, 1.2×10^4 g/mol; number of derivatized styrene groups, 9.7 styrene groups per heparin molecule)[17] and styrenated albumin (molecular weight, 6.6×10^4 g/mol; number of derivatized styrene groups, 15.5 styrene groups per albumin molecule),[16] were prepared according to our previous methods.[16,17] Fibronectin (Fn) and basic fibroblast growth factor (bFGF) were purchased from Koken Co., Ltd., (Tokyo, Japan) and R&D systems Inc., (MN), respectively. Phosphate-buffered saline solution (PBS, pH 7.4) was purchased from Nissui Pharmaceutical Co., Ltd. (Tokyo, Japan). (1*S*)-7,7-Dimethyl-2,3-dioxobicyclo[2.2.1]heptane-1-carboxylic acid (carboxylated camphorquinone, CQ-COOH) was prepared according to the previous paper.[18]

General Method. Visible light irradiation was carried out with a halogen lamp (Tokuso power light with wavelength of illumination 400−520 nm, Tokuyama Co., Ltd., Yamaguchi, and VL-501, LPL Co., Ltd., Tokyo, Japan) and light intensity was measured by a photometer (laser power meter HP-1, Pneum Co., Ltd., Saitama, Japan). X-ray photoelectron spectroscopy (XPS, ESCA-3400, Shimadzu Corporation, Kyoto, Japan) was carried out using a magnesium anode (Mg Kα radiation) under 5×10^{-6} Torr (10 kV, 20 mA) at a 90° takeoff angle. Water wettability of surfaces was evaluated using the sessile drop technique with a contact angle meter (CA-D, Kyowa Kaimen Kagaku Co., Ltd., Tokyo, Japan). The attenuated total reflection (ATR) spectra of the treated surfaces were obtained using a Fourier transform infrared (FT-IR) spectrometer (Spectrum One, Perkin-Elmer Japan Co., Ltd., Kanagawa, Japan) equipped with a ZnSe/diamond reflection element. Fluorescence of the surface was observed with a confocal laser scanning microscope (CLSM, 543 nm excitation; Bio-Rad Lab., Hercules, CA). UV−vis spectra were recorded using a UV-1700 PharmaSpec (Shimadzu Corp., Kyoto, Japan).

Surface Photopolymerization and Characterization. AA Grafting. A typical procedure for surface photograft polymerization is described below. SPU films (1 × 1 cm^2) were immersed in CQ-containing *n*-hexane solution (1 wt %) for 5 min. The surfaces were washed with water and then air-dried. After bubbling with nitrogen, an aqueous AA solution (50 wt %) was poured to a dish (30 mm diameter), on the bottom surface of which a CQ-impregnated SPU film was set. After visible light irradiation (200 mW/cm^2 irradiation intensity) from the top of the dish at 20 °C for 5 min, the SPU film was thoroughly rinsed with water (designated as SPU-AA).

Preparation of Photopolymerized Styrenated Albumin Layer. A typical procedure is described below. The SPU-AA surface was immersed in a solution of styrenated albumin (10 wt %) and CQ-COOH (0.05 wt %) for 12 h to form a liquid film (thickness of approximately 150 μm) on the SPU-AA surface. This was followed by visible light irradiation at 20 °C for 5 min at 200 mW/cm^2 and thorough rinsing with water (designated as SPU-Alb). The photopolymerized surface was immersed in 1-ethyl-3-(dimethylaminopropyl)-carbodiimide hydrochloride (water-soluble carbodiimide, WSC) aqueous solution (1 wt %) for 24 h at room temperature, followed by subsequent thorough rinsing with water and air-drying (designated as SPU-Alb (WSC)).

The amount of albumin in a polymerized layers on surfaces was assayed by Coomassie brilliant blue G-250 (CBBG) staining.[19] Briefly, CBBG aqueous solution was prepared by mixing CBBG (25 mg) in ethanol (12.5 mL, 95%) and phosphoric acid (25 mL, 85% w/v), followed by dilution with water (250 mL). A known concentration of albumin (0.1 mL) was added to the CBBG solution (4 mL) for 10 min, and then centrifuged at 1500 rpm for 20 min. The precipitated albumin−CBBG complex was separated from the CBBG free upper layer. The absorbance of the supernatant at 470 nm was used as the standard calibration curve. The photopolymerized surface (1 × 1 cm^2) was immersed in the CBBG solution (4 mL) for 3 h, and the absorbance of the immobilized albumin was calculated from the measurement of remaining CBBG concentration using the predetermined standard calibration curve.

Preparation of Photopolymerized Styrenated Heparin. A typical procedure is described below. After a solution of styrenated heparin (10 wt %) containing CQ-COOH (0.05 wt %) for 12 h was placed on the SPU-AA surface to form a liquid film (the thickness of approximately 150 μm), it was subjected to visible light irradiation (200 mW/cm^2 irradiation intensity) at 20 °C for 5 min and thorough rinsing with water (designated as SPU-Hep). The photopolymerized surface was immersed in WSC (1 wt %) aqueous solution for 24 h at room temperature, followed by a thorough rinse with water and air-drying (designated as SPU-Hep (WSC)). The amounts of heparin immobilized in the gel layer formed on the surface was assayed using the toluidine blue method.[20,21] Briefly, toluidine blue solution was prepared by mixing toluidine blue (25 mg) with hydrochloric acid (0.01 N) containing NaCl (0.2 wt %). A known concentration of heparin (0.1 mL) was added to the toluidine blue solution (3 mL) for 10 min, and then this was added to *n*-hexane (3 mL). The mixture was shaken to extract the toluidine blue−heparin complex, and the absorbance at 630 nm of lower aqueous layer was measured to determine the amount of noncomplexed toluidine blue. The predetermined linear relationship of the absorbance at 630 nm vs toluidine blue concentration in water was used as the calibration curve to determine the amount of immobilized heparin. The photopolymerized surface (1 × 1 cm^2) was immersed in the toluidine blue solution (3 mL) for 3 h, and the absorbance of the immobilized heparin was calculated using the predetermined standard calibration curve.

Preparation of Photo-copolymerized Styrenated Albumin and Styrenated Heparin Layer. The SPU-AA surface was coated with a solution of styrenated albumin (5 wt %), styrenated heparin (5 wt %), and CQ-COOH (0.05 wt %) for 12 h to form a liquid film (thickness of approximately 150 μm). For immobilization, Fn (10 μg/mL) and/or bFGF (1 μg/mL) were added to the mixed solution. Then, the solution-coated surfaces were irradiated by visible light (200 mW/cm^2 irradiation intensity) at 20 °C for 5 min and thoroughly rinsed with water (designated as SPU-Alb/Hep, SPU-Alb/Fn, SPU-Alb/Hep/Fn, SPU-Alb/Hep/Fn/bFGF). The photopolymerized surface was immersed in WSC (1 wt %) aqueous solution for 24 h at room temperature, followed by thoroughly rinsing with water and air-drying (designated as SPU-Alb/Hep (WSC), SPU-Alb/Fn (WSC), SPU-Alb/Hep/Fn (WSC), SPU-Alb/Hep/Fn/bFGF (WSC)). The amounts of albumin and heparin on the surface were assayed according to the methods described above, respectively.

Surface Characterization. The chemical composition and the wettability of the photopolymerization surfaces were determined by ATR-FTIR and XPS analysis and by water contact angle measurement, respectively.

Measurement of AA-Grafted Layer and Polymerized Heparin Layer. SPU-AA surfaces were immersed in 1 wt % aqueous malachite green solution (0.01 N HCl) for 1 min and washed with water, and then the depth profile of the graft layer stained by malachite green was measured by CLSM (543 nm). The thickness of the polymerized heparin layer prepared as described below was determined by fluorescent dye (DTAF, 5-(4,6-dichlorotriazin-2-yl)amino-fluorescein) coupling to heparin and the cross-sectional view was obtained by CLSM (543 nm). The detailed coupling reaction conditions were described in our previous paper.[22]

Cellular Responses. Platelet Adhesion. Platelet-rich plasma (PRP) was obtained by centrifugation (900 rpm, 15 min, 20 °C) of human whole blood anticoagulated with 3.8% sodium citrate. The substrates were placed on the bottom of a 24-well tissue culture dish (Iwaki Glass Co., Ltd., Chiba, Japan) and were incubated in PRP (5.0 × 10^5 cells/well) for 30 min at 37 °C. After incubation, the substrates were gently washed with PBS. Platelets adhering to the substrates were thoroughly washed with water, freeze-dried, and sputter-coated with platinum. The adhered platelets were observed by SEM.

Endothelial Cell Adhesion and Proliferation. ECs (bovine endothelial cells derived from thoracic aorta) were cultured in Dulbecco's modified Eagle's medium (DMEM, Gibco Laboratories Inc., Grand Island, NY) supplemented

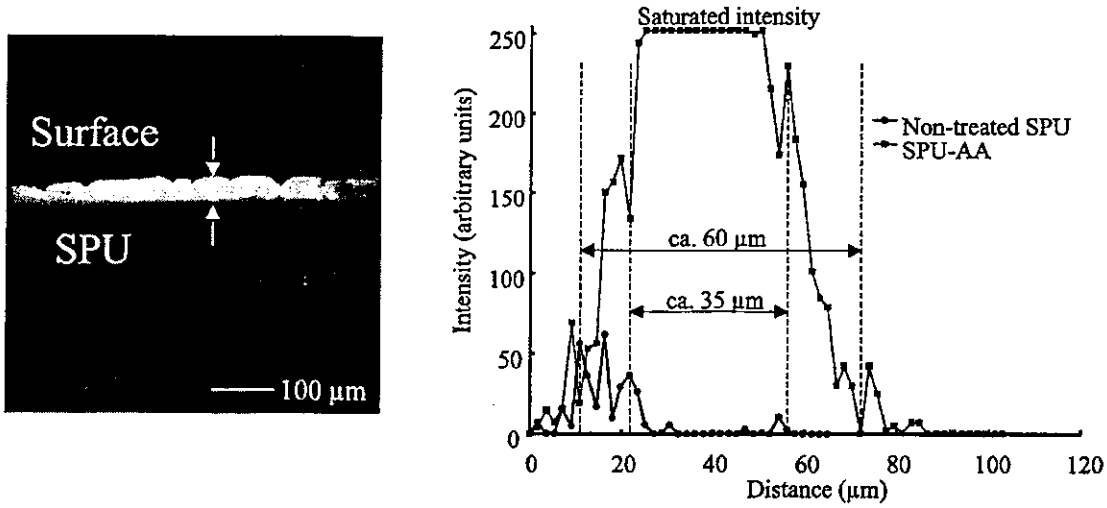

Figure 3. Fluorescence image of polyAA-grafted layer stained with malachite green under CLSM: (A) cross-sectional image; (B) fluorescence intensity plotted against the distance from the outermost surface layer.

Table 1. Surface Elemental Ratio and Water Contact Angle on the Photopolymerized Surfaces

	elemental ratio			contribution of C_{1s} components (%)				water contact angle (deg)	
				C–C	C–O	C=O[a]	C=O[b]		
sample	N/C	O/C	S/C	285.0 eV	286.2 eV	287.0 eV	288.8 eV	advancing	receding
nontreated SPU	0.030	0.26		57.1	39.3		3.6	74.6 ± 1.0	50.5 ± 1.0
SPU-AA	0.001	0.58		41.9	6.1		15.1	40.7 ± 5.9	<10
SPU-Alb	0.115	0.34	0.0045	53.6	25.9	7.2	13.4	89.1 ± 3.0	<10
SPU-Alb (WSC)	0.103	0.32	0.0046	58.5	18.8	14.8	8.0	56.9 ± 3.7	<10
SPU-Hep	0.017	0.38	0.0043	64.0	19.5	13.1	3.5	40.5 ± 2.0	10.3 ± 2.7
SPU-Hep (WSC)	0.047	0.37	0.0067	57.8	12.1	23.4	6.7	24.9 ± 5.1	<10
SPU-Alb/Hep	0.058	0.34	0.0066	53.0	24.0	16.7	6.3	43.7 ± 5.3	<10
SPU-Alb/Hep (WSC)	0.065	0.30	0.0054	58.6	21.8	13.4	6.3	34.2 ± 1.9	20.3 ± 0.7

[a] C=O: CONH, NHCOO (lit. 21). [b] C=O: NHCONH, COO (lit. 21).

with 15% fetal bovine serum (FBS, Gibco Lab., Inc.), 50 IU/mL penicillin, 50 μg/mL streptomycin (Flow Lab., Irvine, Scotland), and 2.5 μg/mL amphotericin B (ICN Biomedicals Inc., Aurora, OH). Cell culture was performed at 37 °C in a humidified atmosphere of 5% CO_2 in an incubator. ECs at passage 4 were used in all the experiments.

Various photopolymerized SPU films were placed on the bottom of a 24-well tissue culture dish (Iwaki Glass Co., Ltd., Chiba, Japan) and ECs (1.0×10^4 cells/well) were seeded and cultured. After a predetermined incubation period, films were gently washed with PBS and then with water, freeze-dried, and sputter-coated with platinum. The relative numbers of adhered ECs were determined from SEM microphotographs.

Separately, ECs were seeded and cultured on poly(ethylene terephthalate) (PET, 15 mm diameter) films that were preadsorbed with 1 wt % albumin or 1 wt % styrenated albumin buffer solution and thoroughly washed with PBS and then placed on the bottom of a 24-well tissue culture dish. The relative numbers of adhered ECs were determined from phase-contrast microphotographs.

Results

Surface Photopolymerization. After 5 min of immersion in 1 wt % CQ containing *n*-hexane solution and subsequent air-drying, SPU films were immersed in degassed 50 wt % AA aqueous solution and irradiated by visible light for a pretermined time (Figure 1-I). The depth profile of the graft layer stained by malachite green was measured by CLSM, and the fluorescence intensity is plotted against the distance from the outermost surface layer (Figure 3). The stained depth was estimated as approximately 60 μm thick. The poly(AA)-grafted SPU surface (SPU-AA) was immersed in styrenated heparin aqueous solution (9.7 styrene groups per molecule), styrenated albumin aqueous solution (15.5 styrene groups per molecule), or its mixture, all of which contained CQ-COOH as water-soluble visible light induced radical generator (Figure 1-II), and then photoirradiated by visible light (Figure 1-III). After thorough washing with water, the photopolymerized surface was immersed in a water-soluble condensation agent (WSC) containing aqueous solution for 24 h to induced covalent bonding between polymerized biomacromolecules mentioned above and between carboxylate groups of SPU-AA and the biomacromolecules (Figure 1-IV).

Table 1 shows surface elemental ratio (determined by XPS analysis) and water contact angles of the treated surfaces at each step. The O/C ratio increased upon surface graft polymerization of AA. Upon photopolymerization of styrenated albumin, N/C ratio was significantly increased. The deconvolution of C_{1s} spectra reveals that higher energy fractions at approximately 287.0 and 288.8 eV, both of which are ascribed to carbonyl carbons,[4] were also significantly

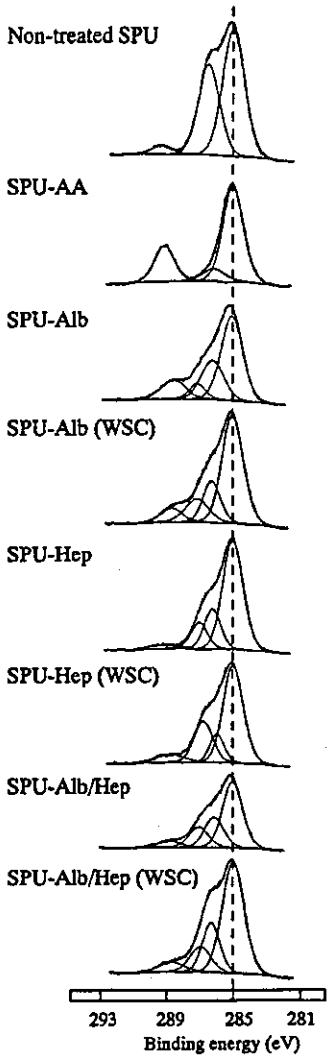

Figure 4. Deconvoluted C_{1s} peaks of XPS spectra of various photopolymerized surfaces.

increased. These indicate that fully albuminated multilayers were fixed on the SPU-AA surface. In addition, the immersion of such a surface in WSC-containing aqueous solution did not change the high N/C ratio and the high subpopulation of the higher energy fractions in the C_{1s} spectra peak. On the other hand, photopolymerization of styrenated heparin (SPU-Hep) reduced N/C ratio but significantly increased O/C ratio. The C—O fraction (at approximately 286.2 eV) ascribed to the ether linkage of the sugar moiety and hydroxyl side chain of heparin molecule in C_{1s} spectra was found to be not high, probably due to hydrocarbon contamination during the sample drying process, which is often observed in hydrophilic polymer surfaces. Photo-copolymerization of styrenated albumin and styrenated heparin and its cross-linking with the polyAA graft chain produced relatively high N/C and O/C ratios and high populations of C—O (at approximately 286.2 eV) and C=O (at approximately 287.0 eV) fractions in the C_{1s} spectra. Despite extensive vigorous washing with water, little spectral difference was observed.

Both advancing and receding contact angles were low as compared with those of nontreated SPU, indicating that polymerized albuminated and heparinized surfaces were highly wettable with water.

Figure 5A shows the ATR-FTIR spectra of photopolymerized surfaces. The spectrum of the SPU-AA surface shows a big shoulder peak at approximately 1730 cm^{-1}, which is assignable to a carboxylic acid group. On the other hand, the spectrum of the photopolymerized albuminated (SPU-Alb (WSC)) surface exhibited a new peak at 1654 cm^{-1},[21] which is due to the secondary amide bond. That of the photopolymerized heparinized surface (SPU-Hep (WSC)) exhibited a new peak at 1050 cm^{-1} that can be ascribed to a sulfate group.[2,21] The spectrum of the mixed albumin/heparin copolymerized (SPU-Alb/Hep (WSC)) surface exhibits both peaks (1654 and 1050 cm^{-1}), the intensities of which were lower than those of the corresponding peaks appearing in spectra of albuminated or heparinized surfaces.

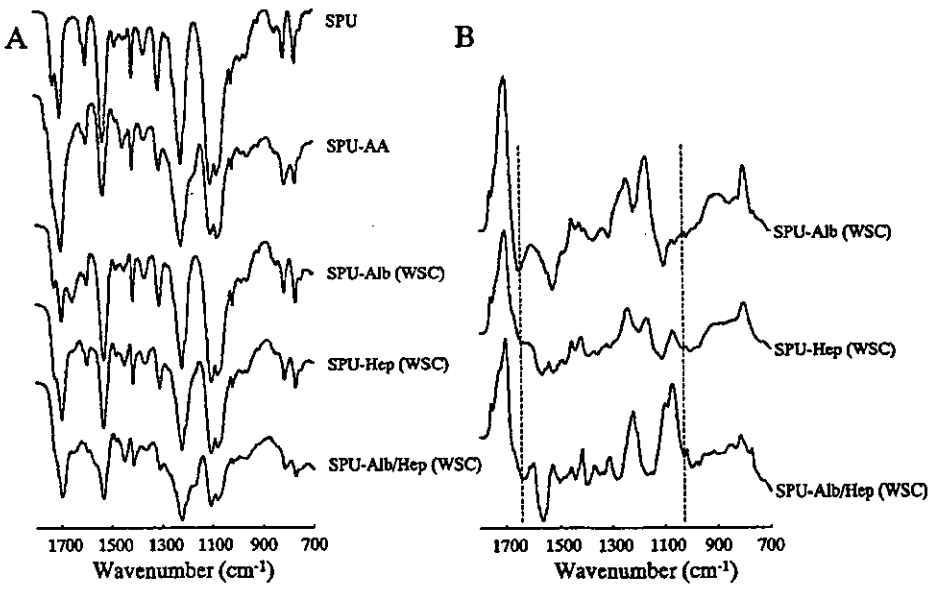

Figure 5. Attenuated total reflection Fourier transform infrared (ATR-FTIR) spectra of various photopolymerized surfaces (A) and difference spectra obtained by subtraction of the spectrum of SPU-AA from respective polymerized spectrum (B).

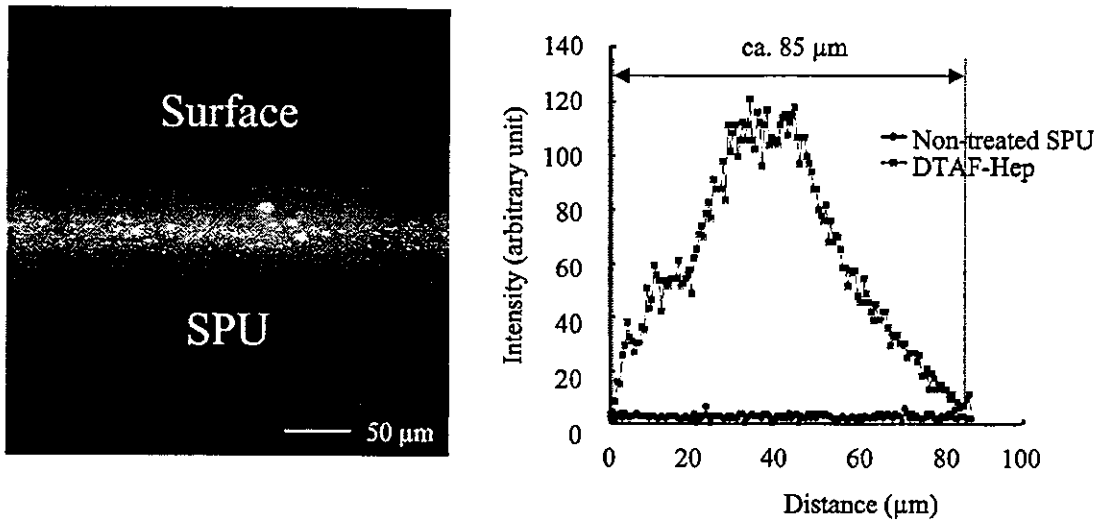

Figure 6. Fluorescence image of polymerized heparin layer containing fluorescent dye (DTAF)-conjugated heparin observed under CLSM: (A) cross-sectional image; (B) fluorescence intensity plotted against the distance from the outermost surface layer.

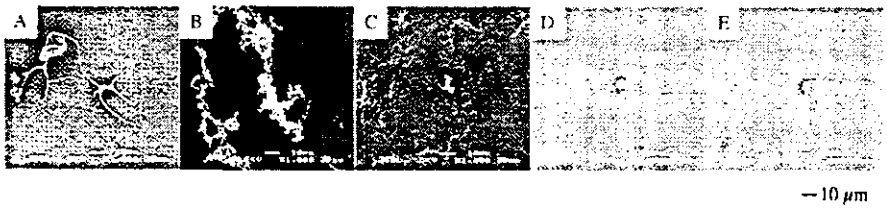

Figure 7. SEM micrographs of photopolymerized surfaces incubated in platelet-rich plasma: (A) nontreated SPU; (B) SPU-AA; (C) SPU-Alb (WSC); (D) SPU-Hep (WSC); (E) SPU-Alb/Hep (WSC).

Table 2. Amount of Albumin and Heparin Immobilized in the PolyAA-Graft Layer Formed on Surfaces ($n = 3$)

sample	amt of albumin ($\mu g/cm^2$)[a]	amt of heparin ($\mu g/cm^2$)[b]
SPU-Alb (WSC)	46.4 ± 3.2	
SPU-Hep (WSC)		26.8 ± 1.5
SPU-Alb/Hep (WSC)	19.7 ± 2.4	12.8 ± 3.6

[a] Measured by coomassie brilliant blue staining. [b] Measured by toluidine blue staining.

This was more clearly observed in the difference spectra obtained by subtraction of the spectrum of SPU-AA from respective polymerized spectra (Figure 5B).

To visualize the thickness of the polymerized heparin immobilized on SPU-AA, immobilized heparin was covalently fixed with a fluorescent dye (DTAF) and measured under CLSM. Figure 6 shows a cross-sectional view of fluorescent heparin layer, which was estimated to be approximately 85 μm in thickness.

The amounts of albumin and heparin polymerized on SPU-AA were determined by dye-complexation methods (CBBG method and toluidine blue method, respectively). After dye complexation in the polymerized layer, the remaining amount of uncomplexed dye in the solution was determined using the predetermined standard curves and is listed in Table 2. The amounts of albumin polymerized in SPU-Alb and SPU-Alb/Hep were estimated as 46.4 ± 3.2 and 19.7 ± 2.4 $\mu g/cm^2$, respectively ($n = 3$). The amounts of heparin polymerized in PU-Hep and PU-Alb/Hep were estimated as 26.8 ± 1.5 and 12.8 ± 3.6 $\mu g/cm^2$, respectively ($n = 3$).

Cellular Responses. Platelet Adhesion: The photopolymerized films were incubated in human platelet-rich plasma for 30 min. Figure 7 shows SEM micrographs of platelet adhesion to photopolymerized surfaces. A large number of adhered platelets and massive aggregation were observed on both nontreated SPU and SPU-AA surfaces. In constrast, a significantly reduced degree of adhesion, spreading, and aggregation of platelets on SPU-Alb, SPU-Hep, and SPU-Alb/Hep surfaces were observed.

Endothelial Cell Adhesion and Proliferation. Bovine endothelial cells (ECs) were seeded and cultured on various polymerized surfaces. Figure 8 shows SEM micrographs of ECs that adhered, spread, and proliferated on these polymerized surfaces. ECs spread and proliferated well on tissue culture polystyrene (TCPS) dishes; in contrast, reduced adhesion and little sign of proliferation were observed for nontreated SPU and slight adhesion and proliferation were observed for the SPU-AA surface. Quantitative data on adhesion and proliferation are given in Figure 9, where the numbers of adhered cells on various polymerized surfaces are plotted against the culture time up to 72 h. Adhesion and proliferation were the least observed for nontreated SPU and SPU-AA. Irrespective of the type of polymerized surface with or without incorporation of cell adhesion protein (fibronectin, Fn) and cell growth factor (bFGF), polymerized surfaces exhibited very good adhesive and proliferative potentials comparable to those of TCPS. The incorporation of Fn into the polymerized albumin surface appeared to enhance cell proliferation. The incorporation of bFGF also enhanced cell proliferation.

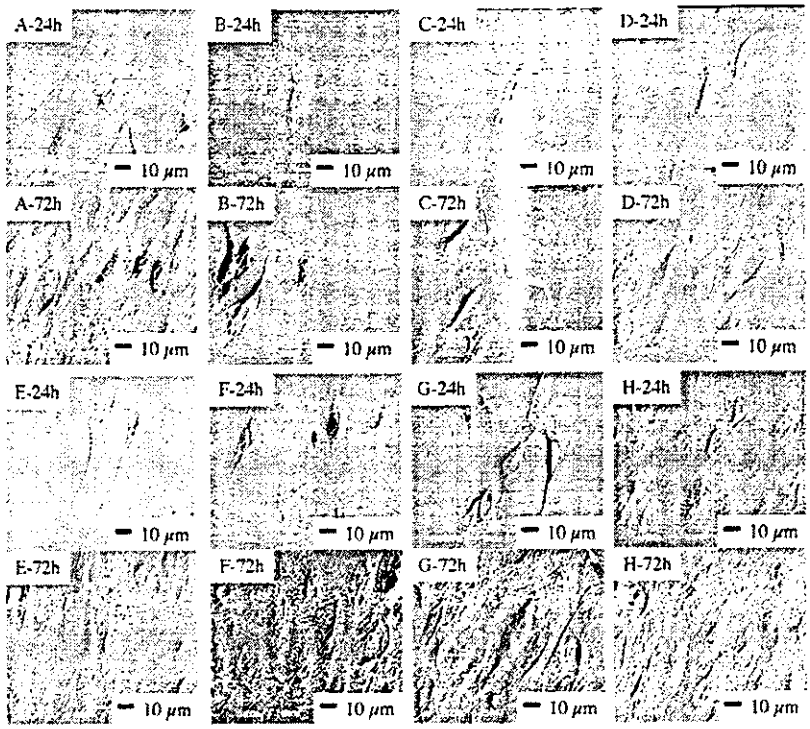

Figure 8. SEM micrographs of bovine endothelial cells cultured on various photopolymerized and covalently fixed surfaces: (A) nontreated TCPS; (B) nontreated SPU; (C) SPU-AA; (D) SPU-Alb (WSC); (E) SPU-Alb/Hep (WSC); (F) SPU-Alb/Fn (WSC); (G) SPU-Alb/Hep/bFGF (WSC); (H) SPU-Alb/Hep/Fn/bFGF (WSC).

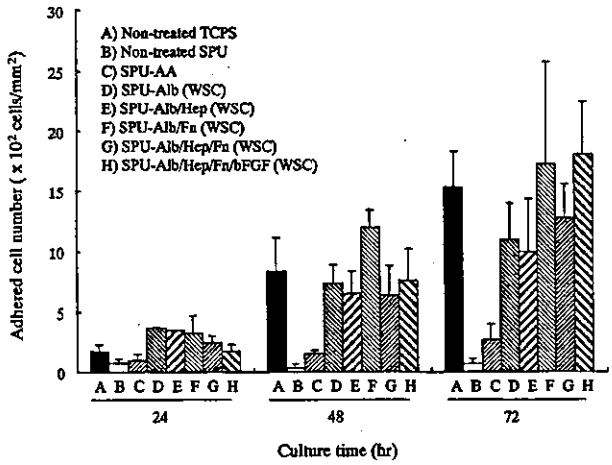

Figure 9. Time-dependent number of bovine endothelial cells adhered on various photopolymerized and covalently fixed surfaces: (A) nontreated TCPS; (B) nontreated SPU; (C) SPU-AA; (D) SPU-Alb (WSC); (E) SPU-Alb/Hep (WSC); (F) SPU-Alb/Fn (WSC); (G) SPU-Alb/Hep/bFGF (WSC); (H) SPU-Alb/Hep/Fn/bFGF (WSC).

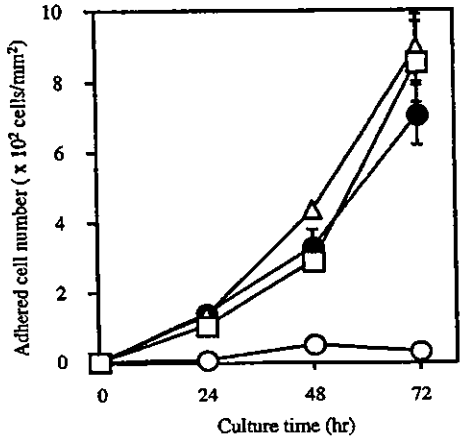

Figure 10. Time-dependent change in number of bovine endothelial cells on surfaces preadsorbed with nontreated TCPS or PET, albumin, or styrenated albumin in PBS (1 wt %) for 3 h: nontreated TCPS (□); nontreated PET (△); albumin (○); styrenated albumin (●).

It is of interest to see whether styrenated albumin surfaces exhibit noncell adhesivity as found for albumin since albumin does not interact with cellular membrane, unlike cell adhesive proteins such as fibronectin. As shown in Figure 10, endothelial cells adhered, spread, and grew well on the styrenated albumin-adsorbed surface, which are comparable to those on nontreated TCPS, whereas little cell adhesion was observed for nontreated albumin as expected. This indicates that styrenated albumin is cell adhesive probably due to increased hydrophobicity derived from multiply derivatized of styrene groups which eventually induce nonspecifically to interact with cell membrane.

Discussion

The realization of normal tissue architecture on a foreign surface is the ultimate task of the development of synthetic and biologic implants. If an artificial implant is densely covered by major components of ECMs, it will be accepted by hostile environment in the body due to minimal foreign-surface-induced activation of humoral body defense mechanisms such as coagulation and complement systems. Sooner or later, cell migration from adjacent tissues and proliferation occur to form a tissue on such a surface. Therefore, this surface may be best suited for cell-incorporated tissue-engineered implants and tissue-contacting artificial implants. Numerous studies have been reported on albumin or heparin

immobilization onto surfaces, aiming at realization of thrombus-free surface for short-term implantation. In general, the albumin-adsorbed surface has been reported to have minimal adhesion of cells including platelets. However, it was reported that the platelet adhesion on the albumin-conjugated surface, which was pretreated with carbon dioxide gas plasma, was significantly high. A marked increase in adhesion of platelets and ECs was also observed on albumin−heparin conjugated surfaces, indicating that such a surface was a suitable for matrix for the EC monolayer. As for platelet adhesion, minimized adhesion observed on albumin-, heparin-, or its mixture-polymerized surfaces observed in this study was quite contrary to the proceeding results, although the surface modification and biomacromolecule-immobilization techniques developed by us quite differ from those in the reported paper. The discrepancy between these results remains unsolved.

The amount of fully monolayered albumin on a surface was reported as 0.1−0.8 $\mu g/cm^2$,[14,24] depending on the configuration of the adsorbed albumin, and that of heparin immobilized on a polyAA-grafted surface, which was induced by plasma glow discharge treatment, followed by thermal polymerization, is 1.23 $\mu g/cm^2$.[4] For the albumin-adsorbed surface, the thickness was estimated to be approximately a few tenths of an angstrom, while that of heparin surface was estimated to be less than a few hundred angstroms.

To increase the thickness of the protein- or polysaccharide-immobilized layer on the surface, our strategy was to utilize visible light induced photopolymerization initiated by radical generation induced by CQ and radical-polymerizable styrenated biomacromolecules which contain at least a few to a few tens of styrene groups per molecule. As for surface photopolymerization, CQ impregnated in SPU generates radicals by hydrogen subtraction from neighboring groups to induced graft polymerization of AA. Upon immersion of the SPU-AA surface in aqueous solution of styrenated biomacromolecules (partially derivatized with 4-vinylbenzoic acid or 4-vinylanilin), adsorption and absorption of these biomacromolecules on and into the polyAA-grafted layer occurred. The adsorption on and absorption into the grafted layer was qualitatively and quantitatively determined by using a dye complexing with or bound to the polymerized biomacromolecules. As shown in Figures 3 and 6, the thickness of the polyAA-grafted layer was estimated to be approximately 35−60 μm, and that of the polymerized heparin layer, which is composed of s-IPN with segmented polyurethane, was estimated to be approximately 80 μm, as determined by CLSM.[23] This quite deep s-IPN structural formation is due to solvent soaking of CQ which penetrates into a deeper region of surface and even bulk phase. Using dye-complexation methods, the amounts of these polymerized biomacromolecules were determined to be approximately 46 $\mu g/cm^2$ for the polymerized albumin layer and 27 $\mu g/cm^2$ for the polymerized heparin layer. The polymerized albumin layer was almost 100 times thicker than the monolayer-packed albumin, which was adsorbed from a dilute aqueous solution. In addition, when a mixed solution of these polymerizable biomacromolecules was mixed with cell adhesive protein such as fibronectin and growth factor such as bFGF, densely proteinaceous multilayers that contain heparin and cytokine were formed by sequential reactions. Thus, a relatively thick biomacromolecule polymerized and co-immobilized layer was formed and covalently coupled on the surfaces grafted with polyAA.

Preliminary experiments of platelet adhesion and endothelial cell adhesion and proliferation encouraged us to utilize such polymerized surfaces for improving blood- and tissue-compatible devices as well as tissue-engineered devices. The co-immobilization of bioactive substances in a biologically derived, thick gel layer may realize sustained release for a long time due to complexation of negatively charged heparin and bFGF, which has cluster of basic amino acid in a molecule. This may realize a continuously stimulating "bioactive" extracellular milieu, thus enhancing tissue morphogenesis including more rapid endothelialization.

Acknowledgment. This study was financially supported by the Promotion Fundamental Studies in Health Science of the Organization for Pharmaceutical Safety and Research (OPSR) under Grant No. 97-15, and in part by a Grant-in-Aid for Scientific Research (A2-12358017, B2-12470277) from Ministry of Education, Culture, Sports, Science, and Technology of Japan.

References and Notes

(1) Park, K. D.; Piao, A. Z.; Jacobs, H.; Okano, T.; Kim, S. W. *J. Polym. Sci.* **1991**, *29*, 1725−1737.
(2) Barbucci, R.; Magnani, A.; Albanese, A.; Tempesti, F. *Int. J. Artif. Organs* **1991**, *14*, 499−507.
(3) Ito, Y.; Sisido, M.; Imanishi, Y. *J. Biomed. Mater. Res.* **1986**, *20*, 1157−1177.
(4) Kim, Y. J.; Kang, I. K.; Huh, M. W.; Yoon, S. C. *Biomaterials* **2000**, *21*, 121−130.
(5) Olsson, P.; Sanchez, J.; Mollnes, T. E.; Riesenfeld, J. J. *J. Biomater. Sci. Polym. Ed.* **2000**, *11*. 1261−1273.
(6) Matsuda, T.; Magoshi, T. *Biomacromolecules* **2001**, *2*, 1169−1177.
(7) Kottke-Merchant, K.; Anderson, J. M.; Umemura, Y.; Merchant, R. E. *Biomaterials* **1989**, *10*, 147−155.
(8) DeQueiroz, A. A. A.; Barrak, E. R.; Gil, H. A. C.; Higa, O. Z. *J. Biomater. Sci. Polym. Ed.* **1997**, *8*, 667−681.
(9) Hennink, W. E.; Dost, L.; Feijen, J.; Kim, S. W. *Trans ASAIO* **1983**, *29*, 200−205.
(10) Brynda, E.; Houska, M. *J. Colloid Interface Sci.* **1996**, *183*, 18−25.
(11) Brynda, E.; Housla, M.; Jirouslova, M.; Dyr, J. E. *J. Biomed. Mater. Res.* **2000**, *51*, 249−257.
(12) Bos, G. W.; Scharenborg, N. M.; Poot, A. A.; Engbers, G. H.; Beugeling, T.; Aken, W. A.; Feijen, J. *J. Biomed. Mater. Res.* **1999**, *47*, 279−291.
(13) Adms, J. C.; Watt, F. M. *Development* **1993**, *117*, 1183−1198.
(14) Matsuda, T.; Takano, H.; Hayashi, K.; Taenaka, Y.; Takaichi, S.; Umezu, M.; Nakamura, T.; Iwata, H.; Nakatani, T.; Tanaka, T.; Takatani, S.; Akutsu, T. *Trans. ASAIO* **1984**, *30*, 353−358.
(15) Ziani-Cherif, H.; Abe, Y.; Imachi, K.; Matsuda, T. *J. Biomed. Mater. Res.* **2002**, *59*, 386−389.
(16) Nakayama, Y.; Okuda, K.; Matsuda, T. Under preparation.
(17) Matsuda, T.; Magoshi, T. *Biomacromolecules*, in press.
(18) Nakayama, Y.; Mukai, T.; Hirano, Y.; Matsuda, T. Under preparation.
(19) Sedmak, J. J.; Grossberg, S. E. *Anal. Biochem.* **1977**, *79*, 544−552.
(20) Smith, P. K.; Mallia, A. K.; Hermanson, G. T. *Anal. Biochem.* **1980**, *109*, 466−473.
(21) Kang, I. K.; Kwon, O. H.; Lee, Y. M.; Sung, Y. K. *Biomaterials* **1996**, *17*, 841−847.
(22) Gohda, M.; Magoshi, T.; Kato, S.; Noguchi, T.; Yasuda, S.; Nonogi, H.; Matsuda, T. *Biomacromolecules* **2001**, *2*, 1178−1183.
(23) Matsuda, T.; Magoshi, T. Under preparation.
(24) Andrade, J. D. *Principles of Protein Adsorption, in Surface and Interfacial Aspects of Biomedical Polymers*; Plenum Press: New York, 1985; Chapter 1, Vol. 2.

BM0200377

Liquid acrylate-endcapped biodegradable poly(ε-caprolactone-*co*-trimethylene carbonate). I. Preparation and visible light-induced photocuring characteristics

Manabu Mizutani, Takehisa Matsuda
Department of Bioengineering, National Cardiovascular Center Research Institute, 5-7-1 Fujishiro-dai, Suita, Osaka 565-8565, Japan

Received 29 November 2001; revised 14 February 2002; accepted 14 February 2002

Abstract: Photocurable liquid biodegradable copolymers were prepared by ring-opening copolymerization of ε-caprolactone (CL) and trimethylene carbonate (TMC) in the presence of a multifunctional hydroxyl group-bearing substance (di-, tri-, and tetra-functional alcohol and poly(ethylene glycol) (PEG) and its four-branched derivative) as an initiator and subsequent endcapping with acryloyl chloride at their hydroxyl terminals. These multifunctional, viscous liquid copolymers (molecular weights; approximately 2×10^3 to 7×10^3 g/mol) were converted to crosslinked solids by visible-light irradiation in the presence of camphorquinone as an initiator. The photocuring rate of these copolymers was enhanced by both higher functionality and lower molecule weight of the copolymers used. The photocuring rate depended on the amount of reducing agent (methacrylic acid 2-dimethylaminoethyl ester). Upon immersion in a phosphate buffer solution (pH 7.4), hydrolysis occurred preferentially on the surface except for photocured PEG-based copolymers that were degraded faster via both surface erosion and bulk degradation than low molecular weight alcohols-based copolymers. Cylindrical photocured constructs prepared by photoirradiation to the whole body in a mold filled with the liquid copolymer was demonstrated as an example of shape fabrication of biodegradable biomedical devices. © 2002 Wiley Periodicals, Inc. J Biomed Mater Res 62: 387–394, 2002

Key words: photocuring; visible light; hydrolysis; ε-caprolactone; trimethylene carbonate; camphorquinone; surface erosion; bulk degradation

INTRODUCTION

Hydrolytically degradable (*co*)polymers have been extensively studied in the field of biomaterials for use as matrix components of controlled release devices, degradable sutures, absorbable fibers, and implants for bone fixation.[1–5] Because these are biodegraded during the course of implantation, irrespective of bulk degradation or surface erosion, artificial implants will be degraded and sorbed, and will finally disappear to be replaced with regenerated tissues. This is the scenario of "ideal" wound healing with devices made of biodegradable polymers. In general, fabrication of devices has been conducted by conventional techniques, such as solution casting, spinning, molding, or extrusion. Biodegradable polymers are also basic materials for matrix, template, and scaffold for tissue-engineered devices.

If a biodegradable liquid polymer or prepolymer is subjected to liquid-to-solid transformation under photoirradiation, a very fine-structured device design and a precise surface architecture for biocompatible designs and artificial organs are feasible in principle, because photoreaction occurs only at the irradiated portion and during the irradiation time. Furthermore, injection of such a liquid prepolymer into the body and subsequent photoirradiation may form an *in situ* construct for diseased or damaged tissues.[6–8]

In our previous studies, we reported the preparation of photocurable, biodegradable, liquid copolymers, poly(CL/TMC)s, which are composed of ε-cap-

Correspondence to: T. Matsuda, Department of Biomedical Engineering, Graduate School of Medicine, Kyushu University, 3-1-1 Maidashi, Higashi-ku, Fukuoka 812-8582, Japan; e-mail: matsuda@med.kyushu-u.ac.jp

Contract grant sponsor: Johnson & Johnson Medical Japan (Tokyo, Japan) (to M.M.)
Contract grant sponsor: Promotion of Fundamental Studies in Health Science of the Organization for Pharmaceutical Safety and Research (OPSR); contract grant number: 97-15

rolactone (CL) and trimethylene carbonate (TMC) and have photodimerizable groups, coumarin, at their terminals [designated as coumarin-endcapped poly(CL/TMC)].[9–11] Upon ultraviolet (UV) light irradiation, a photocured thin film was obtained. Examples were given for microarchitectural surface coatings with multiple microarrays on one surface. UV light-induced photocuring via intramolecular and intermolecular photodimerization between coumarin groups proceeds only in very thin liquid films because UV light is absorbed by most organic materials. In addition, photodimerization reactions or curing proceeded very slowly because only an associated pair of coumarin groups undergoes dimerization.[9–14]

If photocuring of liquid materials proceeds via radical polymerization that is induced by visible light irradiation, much thicker liquid film should be photocured rapidly. Therefore, visible light-induced photocurable system may find more versatile applications than UV-induced photocurable systems.

To this end, we devised a visible light-induced photocurable system composed of acrylate-endcapped, biodegradable, liquid copolymers composed of CL and TMC, and camphorquinone as an initiator, which has been used for photocuring of dental resins for many years. In this article, the photocuring system developed is described, and the hydrolytic behavior of photocured copolymers was evaluated *in vitro*.

EXPERIMENTAL

General procedure

All the solvents and reagents were purchased from Wako Pure Chemical Industries, Ltd. (Osaka, Japan) or Sigma-Aldrich Japan, Inc. (Tokyo, Japan). Diglycerol polyoxyethylene glycol ether (b-PEG) was obtained from Shearwater Polymers, Inc. (Alabama, USA). TMC was prepared in our previously report and recrystallized from a mixed solvent of ethyl acetate and hexane.[9] Trimethylolpropane and pentaerythritol were recrystallized from acetone. Other solvents and reagents were purified by distillation. ^{1}H-NMR spectra were recorded on a JEOL JNM-GX270 FT-NMR spectrometer (270 MHz, Tokyo, Japan). The chemical shifts were given as δ values using Me_4Si, as the internal standard. IR spectra were recorded on a Shimadzu DR-8020 FT-IR spectrophotometer (Kyoto, Japan). UV absorption spectra were recorded on a JASCO Ubest-30 UV/VIS spectrophotometer (Tokyo, Japan). The number-average molecular weight (M_n) of a polymer was determined by GPC analysis, which was carried out on a Toso SC-8020 (Tokyo, Japan) using poly(ethylene glycol) (PEG) standard. Visible light irradiation was carried out on a TOKUSO Power Lite (xenon lamp with UV and IR cut-filter, Tokyo, Japan). The topographic changes of surfaces of a photocured film were determined by a scanning electron microscope (SEM; JEOL JSM-6301F, Tokyo, Japan).

Synthesis of poly(CL-*co*-TMC) copolymer [poly(CL/TMC)]

The preparation of poly(CL/TMC)s were carried out according to the method reported previously.[9,15–20] Briefly, a reaction mixture of 0.33 *M* tin(II)2-ethylhexanoate solution in toluene (125 μL, 43 μmol), trimethylene glycol (7.36 g, 96.7 mmol), TMC (64.0 g, 627 mmol), and CL (71.8 g, 629 mmol) was stirred for 8 h at 180°C in N_2 atmosphere. After vacuum distillation of unreacted monomers, the copolymer, poly(CL/TMC) (**2a**), was isolated by precipitation in methanol. The yield was 139.0 g (99%). $M_n = 2.2 \times 10^3$ g/mol (eluent, DMF). FTIR (KBr, cm^{-1}) 3529, 2955, 2866, 1744, 1252, 1164, and 1036. ^{1}H-NMR (270 MHz, $CDCl_3$, ppm) δ = 1.37 (multiplet), 1.62 (multiplet), 2.01 (multiplet), 2.27 (multiplet), 3.68 (multiplet), and 4.20 (multiplet).

Synthesis of acrylated poly(CL/TMC)

A typical procedure for preparation is as follows. The mixture of (**2a**) (16.6 g, 6.64 mmol) and acryloyl chloride (3.61 g, 39.8 mmol) was stirred for 4 h at 50°C in N_2 atmosphere. The resulting acrylated copolymer of (**2a**) was isolated and purified by the removal of hydrochloric acid and unreacted acryloyl chloride under reduced pressure and the subsequent precipitation in methanol. The yield was 16.9 g (95%). The acrylate contents were determined from the relative peak intensities between the vinyl group of acrylated copolymer and methylene groups ascribed to the coumarin group of coumarinated copolymer used as a reference compound at the same concentration. (The coumarin content of coumarinated copolymer was quantitatively determined by UV spectroscopy in our previous article.[9]) in ^{1}H-NMR spectra. The vinyl content was determined as 8.1×10^{-4} mol/g. FTIR (KBr, cm^{-1}) 2950, 2868, 1739, 1614, 1250, 1167, and 1038. ^{1}H-NMR (270 MHz, $CDCl_3$, ppm) δ = 1.37 (multiplet), 1.62 (multiplet), 2.01 (multiplet), 2.27 (multiplet), 4.20 (multiplet), 5.82 (multiplet), 6.13 (multiplet), and 6.38 (multiplet).

Visible light-induced photocuring characteristics

A mixed liquid film of acrylated copolymer and camphorquinone, coated on a cover glass, was irradi-

ated with visible light (80 mW/cm^2 at 488 nm). After immersion in dichloromethane to dissolve the solvent-dissoluble part, the insoluble copolymer was weighed. The photocuring yield was defined as the weight percentage of the insoluble part (W_g) against that of the coated copolymer (W): $W_g/W \times 100$.

Water adsorptivity

Each photoirradiated, round-shaped film of the acrylated copolymer (diameter 15 mm and 0.3 mm thickness) was immersed in water for 2 days at room temperature. The degree of water adsorptivity (DW) was determined as the relative amount of water uptake against the copolymer at the equilibrium state.

Hydrolytic behaviors

The determination of hydrolytic degradation characteristics of photocured films was carried out by measuring the mass changes. A photocured film (diameter 15 mm and 0.3 mm thickness) was weighed and immersed into 0.01 M PBS (phosphate buffered solution) of pH 7.4 at 37°C that was replaced with freshly prepared solution every week for up to 4 weeks. After 1 week, the films were dried and weighed, and immersed in a freshly prepared buffer solution. Before and after 4 weeks of immersion, the surfaces of the samples were observed under SEM.

Fabrication of macrostructured architecture

Tubular photoconstructs were prepared by photofabrication upon photoirradiation to molds. The photoreactive liquid copolymer, which was poured into an interspace between coaxial double glass tubes composed of different inner diameter of sheath and outer diameter of the inner mandrel (diameter, mandrel/sheath: 1/2, 2/3, and 3/4 mm/mm), was irradiated for 1 min. Upon removal from the double tubes, a cylindrical transparent photoconstruct was obtained.

RESULTS

Preparation of acrylated poly(CL/TMC) copolymers

Acrylate-endcapped copolymers, acrylated poly(CL/TMC)s, were prepared by two-step reactions. The first step is ring-opening copolymerization of CL and TMC in the presence of a di-, tri-, or tetrafunctional low molecular-weight alcohol (trimethylene glycol, trimethylolpropane, or pentaerythritol), poly(ethylene glycol) (PEG), or a four-branched PEG derivative (b-PEG) as an initiator, and the second step is esterification of the hydroxyl terminal groups using acryloyl chloride (Scheme 1). Table I lists reaction conditions and compositions and molecular weights of copolymers. As for the first step, the copolymerizations were carried out at the equimolar feed ratio of CL and TMC according to the method reported previously.[9] The molar ratio of the monomer to the hydroxyl group of the initiator was fixed at 6.6 except for **2b** (Table I), and the reaction was allowed to proceed until completion (yield: almost 100%). The compositions of all the copolymers thus prepared, as determined by ^{1}H-NMR spectroscopy, were almost equimolar as expected (Table I). All the resulting copolymers were viscous liquids. The esterification carried out at the excess amount of acryloyl chloride against the hydroxyl group resulted in full esterification, which was confirmed by IR and ^{1}H-NMR spectroscopies. The vinyl contents, determined by ^{1}H-NMR spectroscopic measurement using the corresponding reference copolymers, were listed in Table I.

Visible light-induced photocuring

Photopolymerization induced by visible light (UV and IR cut filter-attached xenon lamp as a light source)

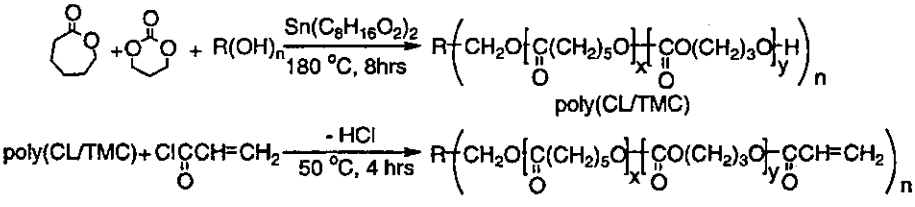

$R(OH)_n$: n	low-mol.-wt. alcohol	hydrophilic poly(ethylene glycol) derivative
2	trimethylene glycol	poly(ethylene glycol) (mol. wt. 1000)
3	trimethylolpropane	
4	pentaerithritol	diglycerol polyoxyethylene glycol ether (mol. wt. 2040)

Scheme 1. Preparation of photoreactive poly(CL/TMC).

TABLE I
Acrylated Liquid Copolymers

Polymer Code Name	Initiator R(OH)$_n$	n[a]	Fraction[b]	Poly(CL/TMC) M_n[c]	CL:TMC	Acrylated Copolymer Content[d] (mol/g)	M_w[e]	DW[f]
2a	$CH_2(CH_2OH)_2$	2	6.6	2.2×10^3	0.50:0.50	8.1×10^{-4}	2.5×10^3	0.01
2b	$CH_2(CH_2OH)_2$	2	13.2	4.3×10^3	0.49:0.51	4.0×10^{-4}	5.0×10^3	0.01
2c	PEG1000	2	6.6	3.3×10^3	0.52:0.48	5.7×10^{-4}	3.5×10^3	0.32
3a	$CH_3CH_2C(CH_2OH)_3$	3	6.6	3.5×10^3	0.51:0.49	8.1×10^{-4}	3.7×10^3	0.01
4a	$C(CH_2OH)_4$	4	6.6	5.3×10^3	0.49:0.51	8.1×10^{-4}	5.0×10^3	0.01
4b	b-PEG[g]	4	6.6	7.4×10^3	0.49:0.51	5.7×10^{-4}	7.0×10^3	0.32

[a]Multifunctionality of initiator.
[b]Molar fraction of monomer per total OH groups.
[c]Number-average molecular weight of nonmodified copolymer determined by GPC (PEG Standard).
[d]Acrylate content determined by using the corresponding reference copolymers.
[e]Molecular weight determined based on acrylate content.
[f]Degree of water adsorption of photocured film (relative weight of water uptake to polymer).
[g]Diglycerol polyoxyethylene glycol ether) (mol. wt. 2040) purchased from Shearwater, Inc.

was carried out in the presence of camphorquinone as the initiator at different camphorquinone concentrations. The photocured copolymers, which were not soluble in any organic solvent, were obtained, irrespective of copolymers. Figure 1 shows the dependence of photocuring on irradiation time and on camphorquinone concentration for the photoreactive copolymer (**4a**). The photocuring yield (defined as the weight percentage of the insoluble part against the initial weight of liquid) increased with both photoirradiation time and camphorquinone concentration. At higher concentrations of camphorquinone (1.0 and 5.0 wt %), there was little difference in the photocuring time course, which is completed after around 30 s of photoirradiation under this experimental condition.

Figure 2 shows acrylate functionality dependence on photocuring using di-, tri-, and tetra-acrylate copolymers, all of which have almost identical chemical composition of TMC and CL but different molecular weight. Photocuring characteristics were enhanced slightly with higher multifunctionality. At the same functionality, a lower molecular weight (mol. wt. approximately 2500 g/mol) of difunctional copolymer slightly enhanced the photocuring rate compared to a higher molecular weight copolymer (mol. wt. 5000 g/mol) (Fig. 3). Copolymers (**2b**) and (**4b**), both of which are based on PEG derivatives, exhibited higher photocuring characteristics than copolymers, (**2a**) and (**4a**), derived from low molecular weight alcohols (Fig. 4).

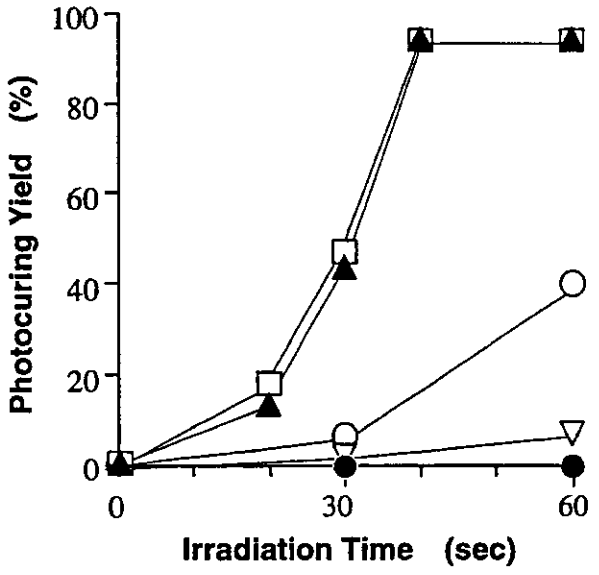

Figure 1. Time-dependent photocuring yield of liquid films of acrylated copolymer (**4a**) at different camphorquinone concentration (none—●), 0.1 (▽), 0.5 (○), 1.0 (▲), and 5.0 (□) wt %) by visible light irradiation. Liquid film thickness: 0.40 mm.

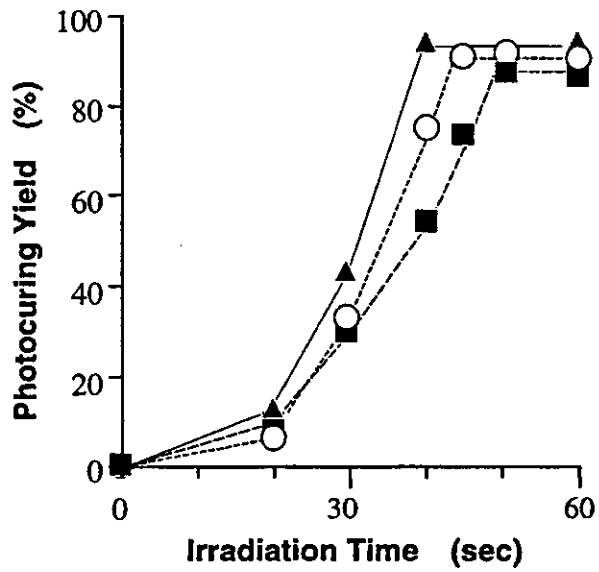

Figure 2. Time-dependent photocuring yield of photoreactive copolymers: (**2a**) (■), (**3a**) (○), and (**4a**) (▲). Camphorquinone concentration: 1.0 wt %. Liquid film thickness: 0.40 mm.

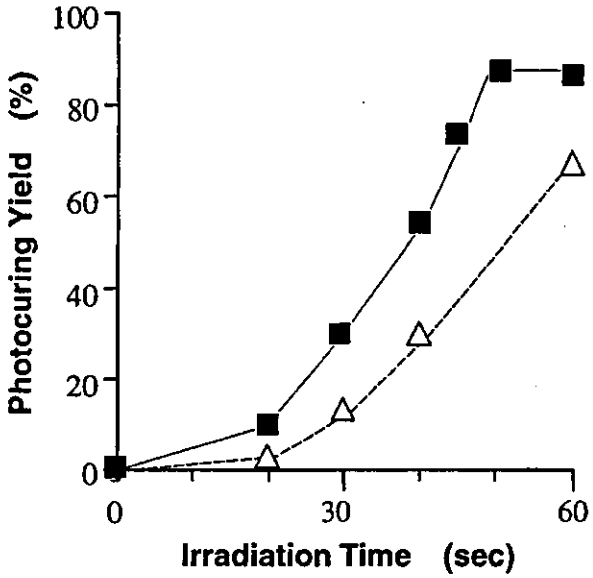

Figure 3. Time-dependent photocuring yield of photoreactive copolymers: (2a: M_n 2.5 10^3) (■), and (2b: M_n 5.0 × 10^3) (△). Camphorquinone concentration: 1.0 wt %. Liquid film thickness: 0.40 mm.

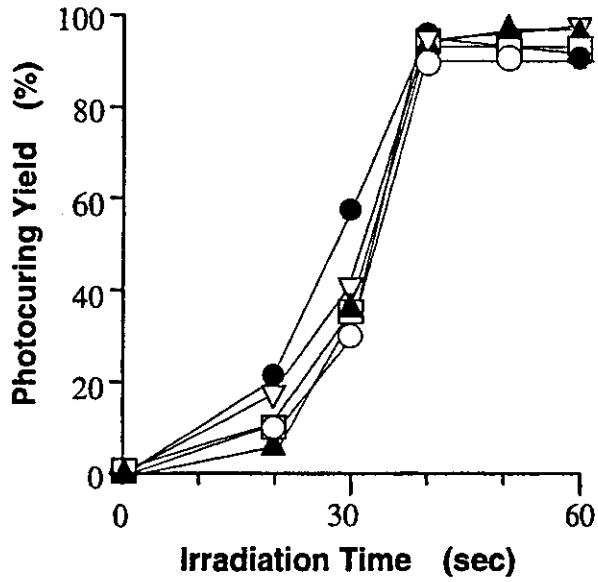

Figure 5. Dependence of photocuring yield of photoreactive copolymer (4a) on liquid film thickness. Camphorquinone concentration: 1.0 wt %. Liquid film thickness: 0.2 (●), 0.8 (▽), 1.6 (□), 5.0 (▲), and 10.0 (○) mm.

The dependency of photocuring yield on the liquid film thickness was examined at thickness ranging from 0.8 to 10.0 mm. Little thickness dependency on the photocuring of liquid film was observed (Fig. 5): complete photocuring occurred after approximately 40 s of photoirradiation, regardless of the thickness under this experimental conditions. The effect of a reducing agent, methacrylic acid 2-dimethylaminoethyl ester, which was added to a polymerizable liquid, was shown in Figure 6. The reducing agent accelerated photocuring at lower concentrations, but appeared to retard photocuring at higher concentrations. All the photocured films obtained were relatively rigid, glassy solid films.

The equilibrium water uptake of photocured co-

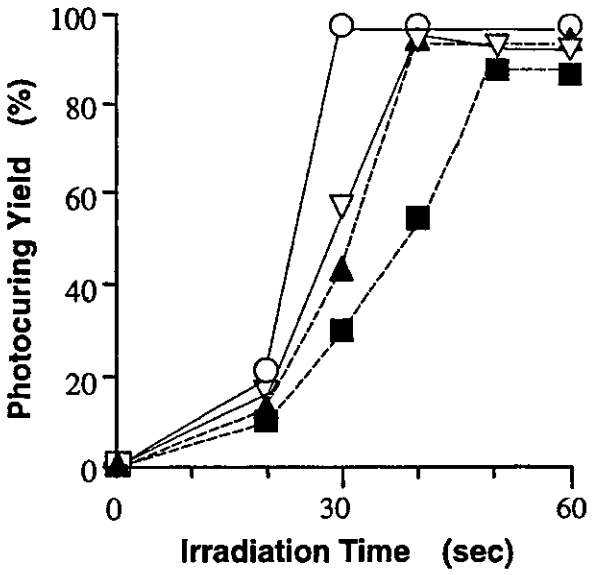

Figure 4. Time-dependent photocuring yield of photoreactive copolymers. (2a) (■) and (2c) (▽) are difunctional and (4a) (▲) and (4b) (○) are tetra-branched copolymers, (2c) and (4b) are PEG-based copolymers. Camphorquinone concentration: 1.0 wt %. Liquid film thickness: 0.40 mm.

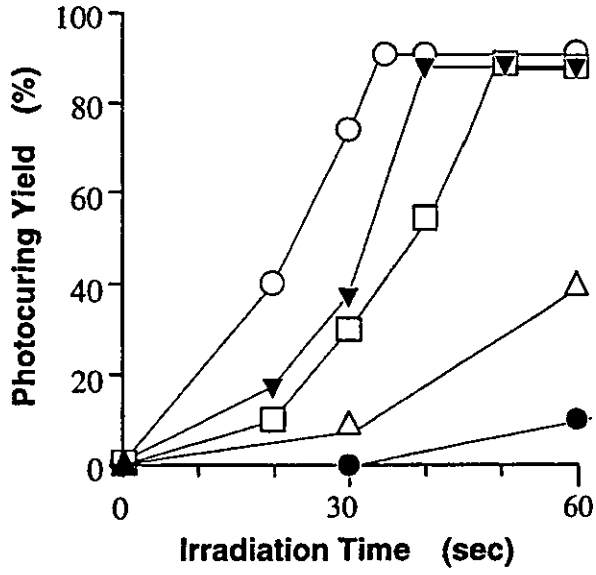

Figure 6. Effect of addition of the reducing agent on photocuring yield of photoreactive copolymer (2a). Concentration of reducing agent, methacrylic acid 2-dimethylaminoethyl ester: 0.0 (□), 0.5 (○), 1.0 (▼),1.5 (△), and 3.0 (●) wt %. Camphorquinone concentration: 1.0 wt %. Liquid film thickness: 0.4 mm.

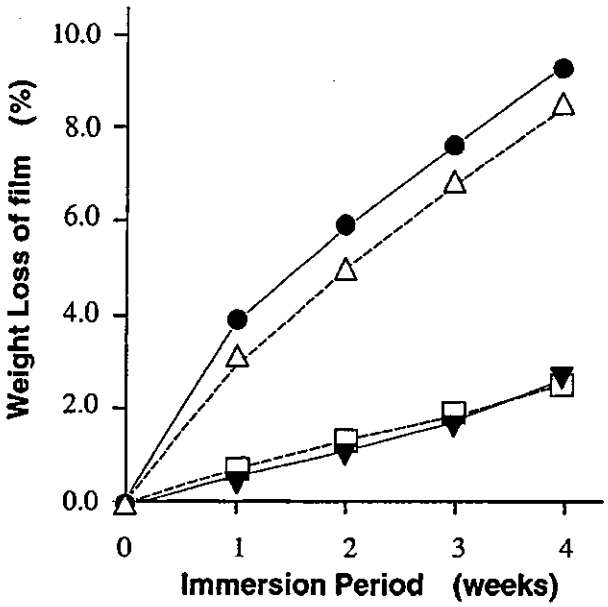

Figure 7. The weight loss of photocured films (diameter 15 mm liquid film, thickness: 0.4 mm) immersed in PBS aqueous solution (0.001 *M*, pH 7.4) at 37°C. (**2a**) (□) and (**2c**) (△) are difunctional and (**4a**) (▼) and (**4b**) (●) are tetra-branched copolymers, (**2c**) and (**4b**) are PEG-based copolymers.

polymers, except for PEG-based ones, was quite small (relative weight of water adsorbed to the photocured copolymer: around a few percentage), but both PEG-based copolymers, (**2b**) and (**4b**), adsorbed water as much as 30% of its weight (Table I).

Hydrolytic behaviors

The hydrolytic behaviors, determined by weight loss upon immersion in the buffer solution (pH 7.4), are shown in Figure 7. The percentage of weight loss of the films increased almost linearly with the immersion time. After 4 weeks of immersion, the photocured films of (**2a**) and (**4a**) showed a few percents of weight loss, whereas PEG-based copolymers, (**2b**) and (**4b**), exhibited higher degradation rates than the former ones (Fig. 7). There was no significant difference in hydrolytic behavior between these di- and tetra-functional copolymers. Figure 8 shows SEM micrographs of samples (**2a** and **2b**) before and after 4 weeks of immersion in PBS (pH 7.4). Although roughened surfaces before immersion were noticed, the very

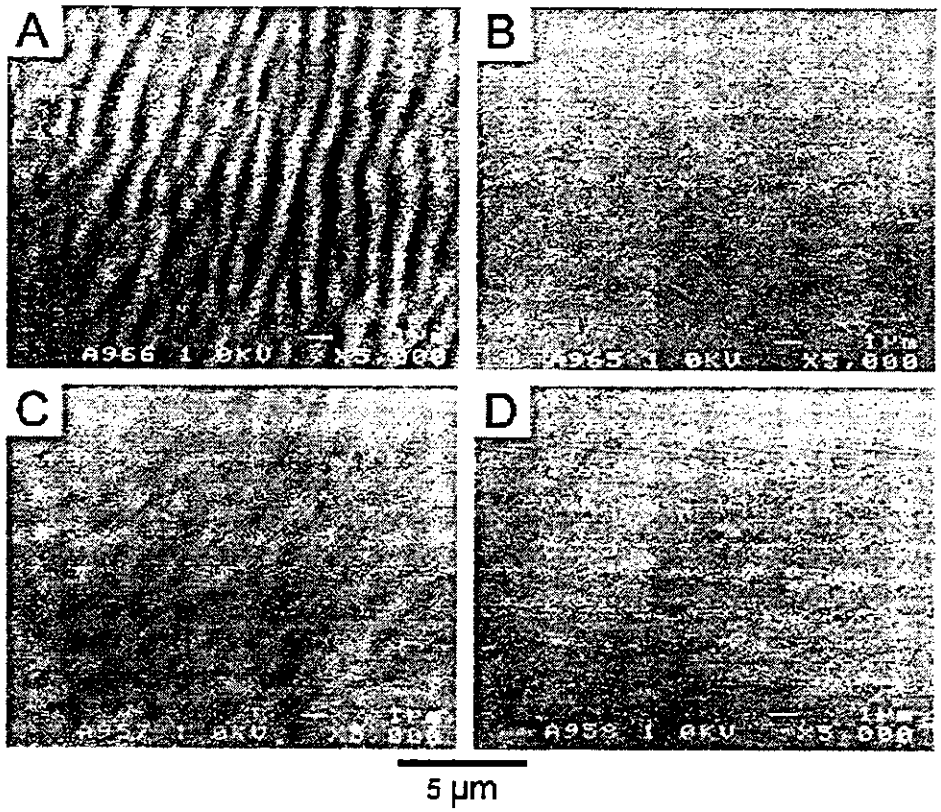

Figure 8. SEM images (×5000) of photocured films of difunctional copolymers: (**2a**) and (**2c**) before and after 4 weeks of immersion in PBS aqueous solution at 37°C. (**2a**) is a trimethylene glycol-based copolymer and (**2c**) is a PEG-based copolymer. (A) (**2a**) and (C) (**2c**): before immersion, (B) (this study was financially supported by the Promotion of Fundamental Studies in Health Science of the Organization for Pharmaceutical Safety and Research (OPSR) under Grant No. 97-15 **a**); and (D) (**2c**): after immersion.

smooth surfaces subjected to hydrolysis may indicate that the hydrolysis occurs preferentially on the surfaces.

Fabrication of macrostructured architecture

The photocuring of a whole body of liquid filled in an interspace of a glass-made coaxial double tube mold composed of a mandrel (inner) and a sheath (outer) produced rigid transparent cylinders (outer diameter: 2–4 mm, wall thickness: 1 mm regardless of models) (Fig. 9). When PEG-derivatized liquid copolymers were used, resultant cylinders were relatively flexible when equilibrated with water.

DISCUSSION

The photoinduced liquid-to-solid transformation has two requirements: the first is that the substance should be in the liquid state before irradiation and the second is that it should possess at least two photoreactive centers in a molecule. We have been extensively studying to develop a series of photocurable liquid copolymers. Polyester–polycarbonate copolymers, composed of CL and TMC, were initially liquid within limited copolymer compositions. In our previous article, the preparation of photocurable, liquid multifunctional poly(CL/TMC) having photodimerizable (coumarin) groups at the molecular terminals as photoreactive centers, and photocharacteristics and hydrolytic behaviors were reported.[9–11] The thin liquid films of copolymers with different functionalities at an almost equimolar copolymer composition of CL and TMC were converted to crosslinked solid films upon UV irradiation. The hydrolytic behaviors *in vitro* and *in vivo* revealed that, except for PEG-based copolymers, which were hydrolyzed at both bulk and surface phases, the hydrolysis of copolymers proceeded in a surface erosion fashion. These conclusions were made based on the results obtained by weekly order hydrolysis, and scanning electron spectroscopic and atomic force microscopic measurements after 1 month of immersion in buffer solution.

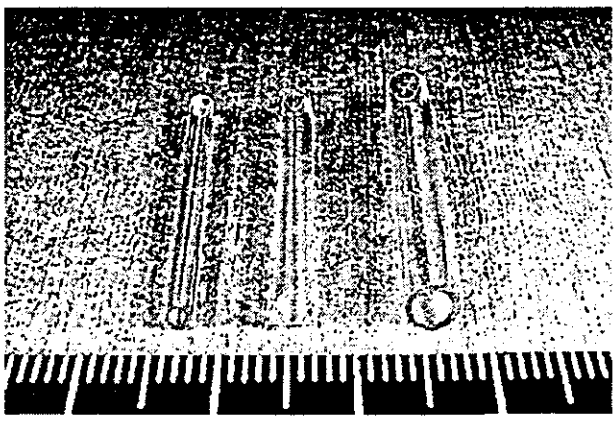

Figure 9. Photographs of cylindrical photocured products by fabrication of microstructured architecture: photocuring mold method. About 3 cm long, and the diameter, inner/outer: 1/2 (left), 2/3 (center), and 3/4 mm (right).

In this study, we devised a visible light-induced photocurable system that contains acrylate group-incorporated poly(CL/TMC)s as a photoreactive center and camphorquinone as the radical-producing agent. These acrylated poly(CL/TMC)s underwent very rapid liquid-to-solid transformation induced by visible light irradiation when camphorquinone is present, compared with the UV-induced photocrosslinking process of coumarin-endcapped poly(CL/TMC), as reported in our previous article.[11] The photocuring yield increased with irradiation time (Fig. 2). The resultant photocured copolymers were insoluble in organic solvent due to crosslinking. Multifunctionality of copolymers gave a large amount of crosslinking (Fig. 2). The photocuring rate was increased with an increase in acrylate content (Fig. 3). PEG-based copolymers exhibited faster photocuring than these low molecular-weight alcohol-based copolymers (Fig. 4). This may be due to the hydrophobic association between the acrylate group and camphorquinone: the hydrophobically associated clusters may be dispersed in the polar PEG-rich matrix. The little thickness dependency upon photocuring, as shown in Figure 5, must be due to a high transparency of the copolymers in the wavelength (λ) region (λ_{max} ascribed to the carbonyl group of camphorquinone: 470 nm). It has been reported that camphorquinone-initiated radical polymerization is greatly accelerated by the addition of tertiary alkylamine such as triethylamine or methacrylic acid 2-dimethylaminoethyl ester.[21–24] Although the exact mechanism involved has not been well understood, the hydrogen abstraction reaction by α-diketone of camphorquinone from a tertiary amine produces a radical anion of camphorquinone and a radical produced in tertiary amine, both of which appear to promote polymerization. In this study, there appears to be an optimal concentration of the reducing agent for acceleration of photocuring, as shown in Figure 6.

Our previous study using coumarinated copolymers showed that hydrolytic degradation of copolymers, obtained using low molecular-weight alcohols as initiators, proceeded via surface erosion mechanism presumably due to quite low moisture uptake characteristics, and that of PEG-based copolymers proceeded via both surface erosion and bulk degradation mechanisms due to high water uptake characteristics.[11] The degradation rate of photocured copolymers in this

study, which was calculated from the slope of weight losses against the immersion period, was equal to that of the coumarin-endcapped copolymer (0.5%/week) reported previously.[11] This observation suggests that surface erosion may proceed for visible light-induced photocured films based on low molecular-weight alcohols. On the other hand, PEG-based copolymers exhibited a degradation rate (2.0%/week) comparable to those of coumarinated copolymers (2.5%/week). This also indicates that, for those copolymers, both surface erosion and bulk degradation simultaneously occurred as is similar to coumarinated ones. As shown in Figure 9, the photocuring mold method was suitable for the visible light-induced microstructured fabrication, by which a complex-shaped scaffold for tissue engineering is feasible and microarchitectural devices will be reported in our forthcoming article.

One of the authors (M.M.) appreciates the continuous encouragement of Dr. G. N. Kumar, Dr. S. C. Arnold, and Dr. A. G. Scopelianos (all of whom are from Johnson & Johnson). This study was partially carried out at the Collaboration Station, Kyushu University.

References

1. Piskin E. Biodegradable polymers as biomaterials. J Biomater Sci Polym Ed 1994;6:775.
2. Bezwada RS, Jamiolkowski DD, Lee IY, Agarwal V, Persivale J, Trenka-Benthin S, Erneta M, Suryadevara J, Yang A, Liu S. Monocryl suture, a new ultra-pliable absorbable monofilament suture. Biomaterials 1995;16:1141.
3. Hutmacher D, Hurzeler MB, Schliephake H. A review of material properties of biodegradable and bioresorbable polymers and devices for GTR and GBR applications. Int J Oral Maxillofac Implants 1996;11: 667.
4. Jeong B, Bae YH, Lee DS, Kim SW. Biodegradable block copolymers as injectable drug-delivery systems. Nature 1997;388: 860.
5. Lemmouchi Y, Schacht E, Kageruka P, De Deken R, Diarra B, Diall O, Geerts S. Biodegradable polyesters for controlled release of trypanocidal drugs: In vitro and in vivo studies. Biomaterials 1998;19:1827.
6. Hill-West JL, Chowdhury SM, Sawhney AS, Pathak CP, Dunn RC, Hubbell JA. Prevention of postoperative adhesions in the rat by in situ photopolymerization of bioresorbable hydrogel barriers. Obstet Gynecol 1994;83:59.
7. Hill-West JL, Chowdhury SM, Slepian MJ, Hubbell JA. Inhibition of thrombosis and intimal thickening by in situ photopolymerization of thin hydrogel barriers. Proc Natl Acad Sci USA 1994;91:5967.
8. Elisseeff J, Anseth K, Sims D, McIntosh W, Randolph M, Langer R. Transdermal photopolymerization for minimally invasive implantation. Proc Natl Acad Sci USA 1999;96:3104.
9. Matsuda T, Mizutani M, Arnold SC. Molecular design of photocurable liquid biodegradable copolymers. 1. Synthesis and photocuring characteristics. Macromolecules 2000;33:795.
10. Matsuda T, Mizutani M. Molecular design of photocurable liquid biodegradable copolymers. 2. Synthesis of coumarin-derivatized oligo(methacrylate)s and photocuring. Macromolecules 2000;33:791.
11. Matsuda T, Mizutani M. Photocurable liquid biodegradable copolymers: *In vitro* hydrolytic degradation behaviors of photocured films of coumarin-endcapped poly(ε-caprolactone-*co*-trimethylene carbonate). Biomacromolecules. Forthcoming.
12. Moghaddam MJ, Matsuda T. Development of a 3-D artificial extracellular matrix: Design concept and artificial vascular media. ASAIO Trans 1991;37:M437.
13. Kito H, Nakajima N, Matsuda T. Differentiated biocompatible design of luminal and outer graft surface: Photocurable extracellular matrices, fabrication, and cellular response. ASAIO J 1993;39:M506.
14. Moghaddam MJ, Matsuda T. Molecular design of three-dimentional artificial extracellular matrix: Photosensitive polymers containing cell adhesive peptide. J Polym Sci Chem Ed 1993;A31:1589.
15. Albertsson A-C, Eklund M. Synthesis of copolymers of 1.3-dioxane-2-one and oxepan-2-one using coordination catalysts. J Polym Sci Part A Polym Chem 1994;32:265.
16. Scopelianos AG, Bezwada RS, Arnold SC, Gooding RD. Liquid polymer filled envelopes for use as surgical implants. U.S. Pat. #5,411,554 (July, 1993).
17. Scopelianos AG, Arnold SC, Bezwada RS, Roller MB, Huxel ST. Injectable microdispersions for soft tissue repair and augmentation. U.S. Pat. #5,599852 (October, 1994).
18. Bezwada RS, Arnold SC, Shalaby WS. Liquid absorbable copolymers for parenteral application. U.S. Pat. #5,653,992 (April, 1995).
19. Scopelianos AG, Arnold SC, Bezwada RS, Roller MB, Huxel ST. Injectable microdipersions for soft tissue repair and augmentation. U.S. Pat. #5,728,752 (March, 1996).
20. Scopelianos AG, Bezwada RS, Arnold SC. Injectable liquid copolymers for soft tissue repair and augmentation. U.S .Pat. #5,824,333 (November, 1996).
21. Cock WD. Photopolymerization kinetics of dimethacrylates using the camphorquinone/amine initiator system. Polymer 1992;33:600.
22. Fujimori Y, Kaneko T, Nishide H, Tsuchida E. Photoreaction and photoinitiation behavior in the light-cured dental resins. Kobunshi Ronbunshu 1993;50:485.
23. Kucybala Z, Pietzak M, Paczkowski J, Lindén LÅ, Rabek JF. Kinetic studies of a new photoinitiator hybrid system based on camphorquinone-*N*-phenylgline derivatves for laser polymerization of dental restorative and stereolithographic (3D) formulations. Polymer 1996;37:4585.
24. Lindén LÅ. Hybrid photoinitiators based on camphorquinone and co-initiators containing amine groups for curing of dental restorative resins with visible light and laser radiation. Plastics Rubber Compos Process Applic 1997;26:91.